FINITE SLAB TWO-PHASE LIQUID-SOLID TRANSIENT HEAT CONDUCTION WITH TRANSIENT FRONT SHIFT

Charl E Janeke

1967 Master's Thesis

University of Pretoria, S/Africa

Submitted Jan/14 1967

An explicit finite element numerical correlation of a modified Binder-Schmidt (graphical) transient *heat-conduction-in-a-solid-material* methodology morphing heat of solidification/freezing of a two-phase medium via a unique *heat-of-solidification* function & regressive/staged time delay. The results have been verified via analytical (step-function) solutions & an experimental wax model.

The advent of spreadsheets & Pentium-class personal computers opened the door to a unique (hands-on) (computational) gradient mapping-methodology as to the transient heat flow/solidification front in a two-phase medium akin to the formation of the crust of the earth. The model hence found a unique application forty-two years later as to enumerating the rate of formation/chilling of the crust of the earth rationally.

Cj/2009-0814

Finite Slab Two-phase Liquid-solid Transient Heat Conduction with Transition Front-Shift.

By

Charl Emelio Janeke

Submitted in Partial Fulfilment for the M.Sc. (Eng.) (Mechanical). Degree, Engineering Faculty, University of Pretoria.

17th February, 1967.

Thesis first submitted 14th January, 1967

I DECLARE THAT THIS THESIS HEREWITH SUBMITTED BY ME FOR THE DEGREE M.Sc. (ENG.) (MECH.) AT THE UNIVERSITY OF PRETORIA, HAS NOT FORMERLY BEEN SUBMITTED BY ME TO ANY OTHER UNIVERSITY FOR A DEGREE.

C.E. Janeke

C.E. JANEKE.

INDEX.

List/.....

Page

List of Tables.

List of Figures.

15/...

Acknowledgements:

The author wishes to express his sincere gratitude to everyone who has contributed to this work.

****

SYMBOLS AND SUBSCRIPTS

Symbol	Description	Units (Btu, h, °C, °F, ft)	Dimension (LM τT)
$a = \frac{k}{\rho C_p}$	Thermal diffusivity	ft^2 / h	$\frac{L^2}{\tau}$
k	Thermal conduction	Btu/h ft °F	$\frac{ML}{\tau^3 T}$
ρ	Density	lb/ft^3	$\frac{M}{L^3}$
C_p	Heat Capacity	Btu/lb °F	$\frac{L^2}{\tau^2 T}$
$\frac{x}{x}$	Tangential intersection distance	ft	L
Z_h	Heating-side tangential intersection distance	ft	L
Z_c	Cooling-side tangential intersection distance	ft	L
h	Convection coefficient	Btu/h ft^2 °F	$\frac{M}{\tau^3 T}$
h_h	Heating side convection coeff.	Btu/h ft^2 °F	$\frac{M}{\tau^3 T}$
h_c	Cooling side convection coeff.	Btu/h ft^2 °F	$\frac{M}{\tau^3 T}$
$\Delta\tau$	Time interval	h	τ
ϕ, ϑ	Temperature excess	°F, °C	T
t_h	Heating plate temperature	°F, °C	T
t_c	Cooling plate temperature	°F, °C	T
t	Transition temperature	°F, °C	T
Δx	Thickness of slab	ft	L
x	Layer thickness	ft	L
Q	Heat production	Btu/ft^3, h	$\frac{M}{\tau^3 L}$

/ ....

Symbol	Description	Units (Btu, h, °C, °F, ft)	Dimensions (LM τT)
K	Heat production	Btu/lb h	$\frac{L^2}{\tau^3}$
K	Heat of transformation	Btu/lb	$\frac{L^2}{\tau^2}$
1	Liquid state		
2	Solid state		
o	Outside		
i	Inside		
h	Heating side		
c	Cooling side		

Abstract:

In this paper it is attempted to prove that an analytical solution for transient heat conduction based on finite intervals can be obtained rapidly by using a high speed electronic digital computer. The method also lends itself to graphical solution for rapid assessment with high accuracy.

Experimental studies conducted on a wax model to correlate the theoretical computations, is also included in this report.

1. INTRODUCTION.

1.1 General Background.

Heat transfer is one of the most discussed sections of the theoretical science and has contributed to classical developments in the analytical mathematics.

The subject is associated with the present developments in technology and presents an unlimited scope for research and development, as testified by numerous publications. In modern science it is essential that all physical processes can be accounted and predicted for and consequently calculations should be analized analytically where possible and correlated with the practice or experimentally. The introduction of electronic computers opened new fields of theoretical study which was not possible earlier due to the great amount of work characteristic to the particular analytic solution methods.

In the following study dynamic heat flow is studied particularly for a two-phase liquid-solid material of finite thickness. The ultimate result lends itself to solution of practical problems on a digital computer or by means of a graphical construction.

1.1.1 Statement of problem:

Transient heat conduction is one of the many physical phenomena that cannot be solved fully analytically [3] and exact solutions are limited to bounded hypothetical conditions. A classical example can be found in the Navier-Stokes equation [11] for fluid flow.

Although numerous specialised solutions on transient heat conduction exist, it is of a special nature for a specific problem.

The/....

The essence of the problem is the development of a mathematical theory to solve transient heat conduction problems in a bounded two-phase liquid-solid material with transition front shift and to define the scope of application and expected diviations in the application range.

1.1.2 Literature survey:

For conduction, theoretical solutions of the transient conduction problem are limited to second order linear differential equations, and the most commonly known are the temperature distribution charts c Heisler and Gröeber [1], [2], [3] for semi-infinite solids with a convective boundary. Solutions for radiating boundaries have been proposed by Friedman,[10] Mann and Wolf,[10] Abarbanel[10] and Fairal[12], for slabs and cylinders. A more recent investigation by R.D. Zerble and J.E. Sunderland[10] produced a range of charts for one-dimensional temperature distributions in a slab, insulated at one end, and subjected to thermal radiation at the other face, using an analogue computer to find the solution. However, solutions of the Fourier equation for a material with heat scources and sinks are not so readily available.

In their work on heat conduction, Carslaw and Jaeger[5] and HSU[1] discuss solutions of the heat conduction equation for melting and freezing, which has been generalized by Neumann[5]. The application of the solutions are limited to the hypothetical assumptions made to derive exact solutions and except for this special case[5], no analytical technique exists for finding solutions[13].

Landau[14] in a paper "Heat conduction in a melting solid" considered the special case of the melting of a solid when the liquid is removed immediately on formation with the other face insulated. With Gauss's theorem applied to heat conduction,

and/ ....

and with a boundary condition assumption that the heat flux equals the rate of heat flow into the solid plus the rate of heat absorption by melting, Landau derived an analytically exact relationship and with numerical integration, computed charts of characteristic dimensionless functions for this bounded relationship. Forster[15] discusses the intricate calculations required for a finite difference solution with a change of phase.

An approximate mathematical technique utilising the "heat-balance" integral was presented by Goodman[13] to calculate the transition front travel. The analytic expressions are limited to;

a) Fixed boundary temperature
b) given heat flux at boundary
c) heat flux generated aerodynamically or by radiation
d) given heat flux at melting front and melt completely removed
e) heat at boundary given and at zero time melt begin to vapourize.

Comparisons with known solutions have been made.

Goodman also points out the mathematical difficulties encountered with non-linear heat transfer problems, e.g. with change of phase. In the general solution using the heat balance integral, he simplifies the problem by assuming all the solids to be at the melting temperature. Although his present method is capable of taking the temperature distribution in the solid state into account, the equations are considerably more complicated, according to Goodman.

In a paper presented at the "First Symposium on Automation and Computation",[6] L.L. van Zyl of the University of Cape Town demonstrated an electronic analogue method used to study the self heating of fishmeal due to chemical reaction. Although an accuracy of 99% has been claimed, this system has the disadvantage that it

has/ ....

has to be built up and tested for every computation and boundary condition and does not lend itself to repeated calculations and optimising boundary conditions, as will become apparent in the following discussions.

Analogue computer solutions are also discussed by N. Freed and C. Ellis [9], who also accentuated the complexity of a pure analytic solution.

The method adopted in this work is an expansion of the basic Schmidt method[3] for heat conduction in finite intervals and corresponds to the solution of a non-linear second order differential equation. The finite nature of this analysis lends itself to the adoption of a digital computer as the mode of calculation. Although the problem can be solved graphically and statistically, the latter two methods are rather tedious.

The programmed solution can be readily used in any problem and by using small enough intervals and iterating appropriately, any boundary condition can be calculated to a high degree of accuracy and the characteristics optimised.

Further, by using this method and employing the parameters derived in the standard literature,[13],[14] temperature history charts can be plotted for engineering materials in the two-phase region.

In the following basic study of transient heat transfer in the two-phase medium, characteristic phenomena are pointed out and outlined on an analytical basis.

It should be noted that there is an essential difference between the analytical and semi-analytical solutions referred to in this survey, and the proposed method. The first method is a compromise between boundary conditions to make the problem solveable, whereas the latter is a solution of the classical problem with fixed outer boundary and without mass transfer from the material.

Although the graphical solution is tedious to use, the computer

program included in Appendix I can be used for rapid calculations with a high degree of accuracy.

Consequently this work is a unique contribution to the field of heat transfer and can be employed to solve problems which cannot be solved with the existing methods outlined in this survey.

For the sake of clarity, main topics are treated in main body of text. More detailed discussions are relegated for the appendices.

1.2 Outline of theory:

The general differential equation for heat conduction is given by the Fourier equation.

$$\frac{\partial \Theta}{\partial \tau} = a\nabla^2 T + \frac{Q'''}{\rho c_p} \qquad \text{---- (1)}$$

where the symbol Q''' denotes the heat produced/unit volume/unit time of the material.

Rewriting Q''' in terms of X''', heat produced/unit mass/unit time of the material, the equation becomes (Appendix C),

$$\frac{\partial \Theta}{\partial \tau} = a\nabla^2 T + \frac{X'''}{c_p} \qquad \text{---- (2).}$$

In the absence of internal heat sources X''' = Q''' = 0.

The differential operator

$$\nabla = \frac{\partial}{\partial x} + \frac{\partial}{\partial y} + \frac{\partial}{\partial z}$$

and

$$\nabla^2 = \frac{\partial^2}{\partial x^2} + \frac{\partial^2}{\partial y^2} + \frac{\partial^2}{\partial z^2} \qquad \text{----(3).}$$

For one dimension; equation (2) reduces to

$$\frac{\partial \Theta}{\partial \tau} = a\frac{\partial^2 T}{\partial x^2} \qquad \text{----(4).}$$

It/.....

It can be shown (Appendix A) that the latter relationship when written in terms of finite intervals, becomes

$$\Delta T = a \Delta \tau \cdot \frac{\Delta^2 T}{\Delta x^2} \qquad \text{----- (5)}$$

and also for one-dimensional finite layers denoted by m, and isochrones denoted by n, the relationship becomes

$$T = \frac{1}{2} \Delta (\Delta T)$$

and $T_{m,\ n+1} = \dfrac{T_{m+1,\ n} + T_{m-1,\ n}}{2}$

where the quantity $a \dfrac{\Delta \tau}{\Delta x^2} = \dfrac{1}{2}$

The latter expression is the conclusion of the familiar Schmidt graphical method for heat conduction in a one-dimensional thermal homogeneous material.

However, this relationship as such does not apply to problems involving internal heat generation or losses. In transition phenomena, such as melting and solidification of solids and liquids, K is a function of temperature only - the latent heat of solidification or melting being a constant for every material. With other problems the relationship becomes more complicated with K a function of temperature and time. (6)

Writing (2) in terms of finite intervals, the equation becomes

$$\frac{\Delta T}{\Delta \tau} = a \nabla^2 T + \frac{K'''}{Cp}$$

and for one-dimensional conduction

$$\frac{\Delta T}{\Delta \tau} / \ldots\ldots$$

$$\frac{\Delta T}{\Delta \tau} = a \frac{\Delta^2 T}{\Delta x^2} + \frac{K'''}{Cp} \qquad \text{----- (7)}$$

Rewriting into the "Schmidt" form, (7) becomes,

$$\Delta T = \left(\frac{a}{\Delta x^2} \cdot \Delta \tau\right) \cdot \Delta (\Delta T) + \frac{K'''}{Cp} \Delta \tau$$

Substituting again $\dfrac{a}{\Delta x^2} \cdot \Delta \tau = \dfrac{1}{2}$

$$\Delta T = \frac{\Delta (\Delta T)}{2} + \frac{K'''}{Cp} \cdot \Delta \tau$$

Defining $K = K''' \cdot \Delta \tau$ as the heat developed/unit mass, ΔT becomes

$$\Delta T = \frac{\Delta (\Delta T)}{2} + \frac{K}{Cp} \qquad \text{-- (8)}$$

where ΔT is the change in temperature of a layer Δx during a time interval $\Delta \tau$.

But $\Delta T = 0$, on the assumption that there is no temperature change during transition from solid to liquid for the finite incremental layer.

Consequently $\sum_{n=n}^{n=x-i} (T_{m,\ n}) = 0$, which is

the summation of all the hypothetical changes in temperature of the layer m during transition of phase.

Hence/.....

Hence $\sum_{n=n}^{n=n+i} ({}^{T}m, n) = 0 = \sum_{n=n}^{n=n+i} \frac{(\Delta T)_{m,n}}{2} \cdot \frac{K}{Cp}$

$\therefore \sum_{n=n}^{n=n+i} \frac{(\Delta T)_{m,n}}{2} = -\frac{K}{Cp}$

Rewriting in terms of finite slabs,

$$\sum_{n=n}^{n=n+i} \frac{1}{2} ({}^{T}m-1, n \; {}^{-t}m+1, n \; {}^{T+2}m, n) = -\frac{K}{Cp}$$

and for a limited bounded region

$$\frac{{}^{T}m+1, n \; {}^{-T}m-1, n}{2} = {}^{t}m, n+1$$

$$\therefore \sum_{n=n}^{n=n+i} ({}^{-t}m, n+1 \; {}^{-t}m, n) = -\frac{K}{Cp}$$

$$\text{i.e.} \quad \sum_{n=n}^{n=n+i} ({}^{t}m, n+1 \; {}^{-t}m, n) = \frac{K}{Cp} \qquad \text{----- (9)}$$

The latter means that the algebraic sum of the temperature increases at the transition temperature for a specific layer $= \frac{K}{Cp}$, as defined.

This implies that the transition temperature is not kept constant, but in fact varies with a finite amount not more than half of the mean temperature difference of the relevant layers, m - 1, m + 1.

The fluctuations are summed until equation (9) is satisfied. Phase change is only considered for one layer at a time.

Overall error can be decreased by selecting small increments of either time or slab-thickness, by which the introduced error of varying transition

temperature/.....

temperature is limited.

Calculations can be done either graphically (Fig. 5, Appendix 6) or numerically, the latter preferably on a digital computer (Appendix I, 5).

Heat flux is calculated by computing the heat flow for every time increment through the outer and inner layer and summation over the desired time i,

hence $Q_o = \sum_{\substack{n=n \\ m=1}}^{n=n+i} ({}^{T}m, n+1 \; {}^{-t}m+1, n+1) \times \frac{K}{x}$

and

$$Q_i = \sum_{\substack{n=n \\ m=m}}^{n=n+i} ({}^{t}m, n+1 \; {}^{-t}m, n+1) \times \frac{K}{x} \; .$$

1.2.1 Systematic illustration of the method.

The transition formulation can be demonstrated in the following figure:-

Fig.

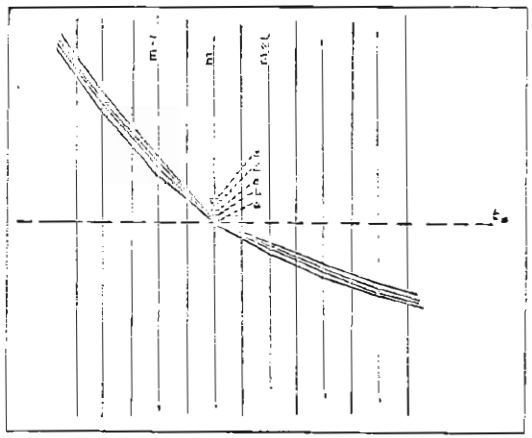

When with heating the computed or graphically solved average (reference) temperature in one layer has reached the melting point the temperature is kept constant at the point a. The temperature increase for the following time interval at the layer m is then computed (Appendix B) and noted, eg. point b, but the subsequent temperature gradient or isocrone through the layer m is diverted back to a. The quantity ab is noted - the defined hypothetical increase in temperature at transition. Subsequent constructions for further time intervals produce the points c, d, etc. When the sum of the hypothetical temperature rises equal the quantity $\frac{\chi}{Cp}$ as defined

(equation/.....

(equation (9)), the transition is complete for the particular layer (m) and the calculations are proceeded with (Appendix B) until the temperature of the next layer (m + 1) reaches the melting point. The transition theorem as illustrated is then repeated for the layer (m + 1) and subsequent layers until the desired solution has been found. The opposite transformation is done for cooling.

1.2.2 Boundary conditions.

Convective boundary conditions are readily accounted for by means of a heat balance, which produces the tangent to the temperature profile (1) and subsequent locus of intersection with the temperature axi as illustrated in Appendix B page 2 and standard literature.

This approach lends itself to simple interpretation of any convective boundary condition combinations as to finite- or infinite-ness, source temperature, heat transfer co-efficient and time dependancy of the latter two functions.

This is done simply by re-evaluating the quantities κ/h and $\vec{U}$, which represent the $x[\tau]$ and $Y[T]$ axis and determine the tangential intersection distance for every time interval, if the boundary conditions are not of a continuous nature.

Subsequently an aperiodic boundary function can be introduced without complicating the demonstrated solution at all. This is definitely an improvement over any pure analytical

solution/.....

solution, which if solveable, becomes extremely complex with engineering boundary conditions.

Radiative boundary conditions can also be evaluated on the foregoing method by introducing the equivalent radiation transfer co-efficient[2], (10)

This implies that the outside temperature for the new temperature isochrone is assumed and the equivalent heat transfer co-efficient calculated or read from a graph.[2]

Hereupon the temperature profile tangential intersection distance $(\frac{k}{h})$ is established, the isochronal gradient computed, and the calculated and assumed values for the wall temperature compared. Following, a new value of wall temperature is chosen. This process is repeated until the iteration error becomes small or negligible. The problem can easily be programmed for a digital computer and solutions rapidly computed on an iteration basis for radiation boundary conditions.

Solution on a digital computer is clearly essential in this case.

For a finite slab, with heating on the outside and cooling on the inside, the intersection distance is also established and the same graphical construction performed as on the outside.

Graphically/.....

Fig.

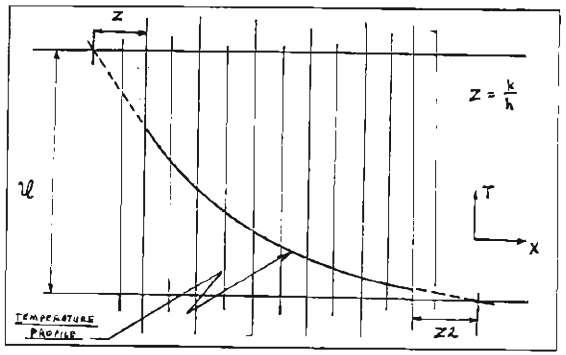

Graphically solved examples are included, figures 5 and 6. It can be clearly seen that with this solution procedure, complex analytical problems, can be rapidly computed and solved on the lines of the relatively simple theoram and visual analysis.

1.2.3 Solution Procedure:

To solve a physical problem of transient heat conduction in a two-phase liquid-solid material with transition front shift, as to transition front travel and temperature gradients at temperature isochrones, the discussed functional characteristics must be derived (figure 3), i.e.

(i) $Z_h = \frac{k}{h_h}, = \frac{k}{h_a}$ (T)

(ii) $Z_c = \frac{k}{h_c}, = \frac{k}{h_a}$ (T)

(iii) $\Delta x \leq Z_h, Z_c$

(iv)/.....

(iv) $\phi = /t - t /, = /t - t / \quad (\tau)$

(v) $\alpha = \frac{k}{\rho C_p}$

(vi) $\Delta\tau = \frac{1}{2} \frac{(\Delta x)^2}{\alpha}$

(vii) $\frac{K}{C_p}$

These quantities are either added to the computer program (Appendix I), or the graphical construction set up by it (figure 6).

Having calculated the required solution, the temperature time history charts can be plotted on a log / linear scale (figure 9 and 10) and corrected as with the demonstrated solutions. Transition front travel is accordingly plotted (figure 7).

With the boundary conditions time and temperature dependant, tangential intersection distance corrections are fed into the solution as the calculation proceeds.

Accordingly numerical solutions are rapidly derived for specific physical problems. In more complicated problems, the basic solution procedure can be used as a subroutine in a comprehensive computer programmed solution.

2./.....

2. Qualitative evaluation of Theoretical Solutions and Experimental Work.

In the foregoing discussion a theory has been outlined with which approximate solution for isochronal temperature gradients and transition front travel can be rapidly achieved for unsteady state heat conduction in a two phase material.

The interpretation of boundary state configuration, steady or unsteady, does not present a major increase in complexity of the solution procedure.

Subsequently, solutions found by using this method for a two-phase wax material will be discussed and compared with experimental results of the same physical configuration. Characteristic phenomena as well as accuracies and limitations of the solution and experimental work are pointed out and compared with other theories and work done in this field (Appendices and references).

2.1 Graphical computations.

Graphical computations have been done for a material with the same physical constants and boundary conditions as the paraffin wax used in the experimental tests (figure 8 and 9, Appendix A.) This could be done because the scope of the tests was initially devised to act as a basis of correlation for the formulated theory outlined in this work. (See also Appendix A, Experimental Work.) Solutions have been obtained for a two-phase material using

the/.....

the physical properties of paraffin wax and the illustrated graphical finite interval method for change of state as outlined in section 1.2 (figure 6, 7 and 11). A single phase solid state mathematical solution for the same material is also included(figures 5 and 13).

A comparison of these results are shown in figure 8 and figure 9. Although the graphical construction seems to be very crude, microscopic results are remarkably accurate, as can be seen from figure 7, where the transition front travel time (derived from figure 6 and 11) is plotted for the experimental results as well as for the graphical solution. There is practically complete correlation, and confirms the quality of the experimental apparatus and results obtained as to transition front travel.

Figure 8 shows a comparison of the temperature increase for layers (1) and (3), solved graphically and experimentally.

From this figure the limitations of the solution are apparent and this is attributed to the finitness of the solution i.e. that the slab is divided into a number of layers (fifteen) and transition is considered for one layer at a time as the melting front proceeds. Physically, this method is true for infinitely small layers and not for finite layers as employed in the solution method. This accounts for the constant temperature when the temperature of a layer reaches the transition temperature. In an infinitely small layer there will clearly not be a constant temperature stage in the heating or

cooling/.....

cooling curve.

In the liquid state correlation with the graphical results, agreement is initially reasonable, but deviation increases with time (layer (1) figure 8).

The solid state shows a deviation for initial layers, which tends to the Schmidt solid state solution shown, but for following layers tends towards the experimental results as time proceeds. It is clear that by taking smaller layers, this error will be decreased and for infinitely small increments will be eliminated.

This phenomena is discussed fully in the next section (2.2) on computed solutions.

Alternatively the error at transition due to finiteness of the finite interval solution(and subsequent constant temperature step)can be corrected on the plotted graph (figure 9) by shifting the solid state melting curve until it reaches the liquid state curve at the transition temperature. The computed results in figure 10 are then similar to the experimental results in figure 11. Corrected results are shown in figure 9, where graphical computed results corresponding with the 1st and 3rd thermocouples are corrected and compared with the experimental results for the 1st and 3rd thermocouples.

In the following figure the correction is illustrated. The curve a b' b c d e denotes the computed solution and the curve

a/.....

a b' c' d' e' the corrected computed solution where b' = c'
= d' = e' and b' is at the transition temperature.

Fig.

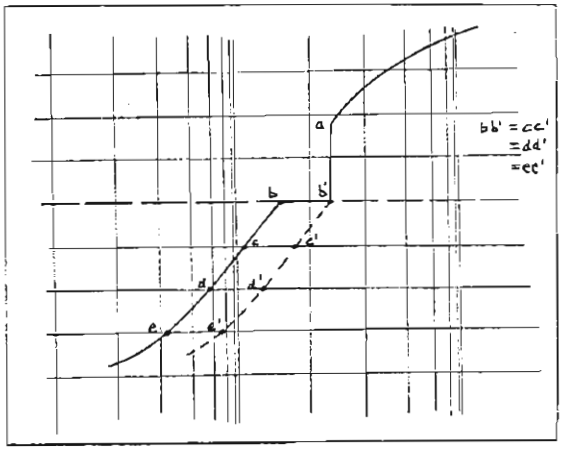

A limitation to the basic solution method is a boundary condition with $Z = \frac{x}{h} = \frac{\gamma}{2}$ numerical (figure 3) because interpolation from the temperature profile to the temperature axis cannot be done and hence subsequent isochrones cannot be computed. In the computed solutions this boundary construction presented a limitation, because the quantity $\frac{x}{h_1} = Z_n$ (figure 3), derived from figure 19, is numerical small. Accordingly small layers were chosen, 15 layers being the least number possible.

An approximation of linear heat flow through the first layer eliminates the boundary construction problem and according solutions are discussed in the next section.

2.2 COMPUTED SOLUTIONS:

Tables 1 - 7 contain solutions computed on an electronic

digital/.....

digital computer using the program in Appendix I, for a range of boundary conditions based on the configuration of the experimental wax model. Results are also plotted in figures 7, 8 and 12.

Table 8 contains a summation of time increments for different layer numbers.

2.2.1 DISCUSSION OF CONTENTS.

Table 1 : This table contains a solution for a 15 layer example similar to the graphical construction and serves as a check on the accuracy of the graphical solution. In figure 7A the results are plotted in the form of transition front travel / time with the experimental and graphical computed curves. Correlation is to within 5% of the three independently solved curves.

As the time increase to equilibrium, it can be seen from figure 7A that the experimentally solved curve deviates away from the computed curve. This can be attributed to the liberation of air in the liquid wax in the form of bubbles accumulating on the heating plate, and the subsequent decrease in contact heat transfer coefficient to the wax during the test.

Figure 8 shows as comparison of experimental, graphical and computed solutions (15 layers).

The/.....

The deviation of the experimental curve away from the graphically solved and computed curves is again apparent as time increases to equilibrium.

Table 2 : This table contains a solution for a boundary condition with $\frac{k}{h} < \frac{\Delta x}{2}$, by taking linear heat flow over the first and last layers and interpolating the temperature curve over two layers. The tangential intersection distance on the temperature axis now becomes $\Delta x = Z_h$ on the heating side and $\Delta x = Z_c$ on the cooling side. Hence any boundary condition can be evaluated using the foregoing approximation.

This table includes a calculation with

$$Z' = Z + \Delta x = 0.33$$

$$\Delta x = 0.3$$

$$Z = 0.03 << \Delta x$$

Figure 7C shows comparative plots.

Table 3 : Calculations are similar to Table 2, except that the boundary conditions are similar to Table 1 for purposes of comparison. Results are plotted in figure 7C.

It/.....

It can be seen clearly from this graph that the error of approximation is less with 30 layers than with 15, and that the curves converge to the experimental plot as time increases.

Table 4 : Calculations for the slab divided into 30 layers for increased accuracy and the results are shown in figure 7A and 7B.

It is significant that a definite displacement exists between the 15 and 30 layer solutions. boundary conditions (figure 7A), which is attributed to the increased accuracy of solution.

Figure 12 shows a comparison of the effect of finiteness for 15 layer and 30 layer solutions. Although there is a displacement due to increased accuracy to corresponding layers, the 30 layer solution is clearly more finite than the 15 layer solution and it can be visualised that by taking an infinite number of layers, the constant temperature steps at transition can be eliminated. Alternatively, correcting for finiteness as illustrated in section 2.1 produces the same result.

Table 5 and 6 : The influence of the latent heat of transformation is studied in these tables. In the literature[4]

the/.....

the heat of transformation for the specific wax fraction is given as the renge 70 - 106 Btu / lb (Appendix H) and in the latter calculations the least value has been used giving $K/_{Cp} = 70^{\circ}$ C. Table 5 is computed for $K/_{Cp} = 126^{\circ}$ C, representing the wax value of k and table 6, for $K/_{Cp} = 98^{\circ}$ C, representing the average value of K through the given range. The results are plotted comparatively in Figure 7B. From the figure follows that the plot where the value of $K/C_p = 98^{\circ}C$, correlation is best with the experimental results and with a further increase in accuracy (number of layers), complete correlation can be expected.

Table 7 : This table is computed for a 5 layer divisor with linear flow approximation in the outer layers.

2.3 Analytical solutions:

An analytical solution for heat transfer in a two-phase material for an infinite slab known as the Neumann solution is described by Carslaw and Jaeger [5] and again by Ständer and Lenhard [6] as an introduction to their own analytical-numerical method also to be discussed in this section.

2.3.1 Neumann Solution.

This solution is based on the Gauss Error Function Theorem which is principally the solution of a 2nd order linear partial differential equation expanded into a power series.

Neumann/.....

Neumann employs this theorem to solve a non-linear second order differential equation, similar to this problem, by setting up two separate linear differential equations for the liquid and solid phase respectively, and considering the non-linearity (change of phase) by a simple heat balance over the transition front. This analysis is discussed in Appendix D.

This unique solution is limited by the assumption made to derive this analytical relationships, ie. an infinite thick layer, a zero reference temperature and the temperature step of heating and cooling. Although the same latter boundary conditions were employed in the present experimental work (Appendix A) and graphical solution (Figure 6), the boundary condition configuration was chosen only as a basis of correlation and not because of a limitation on the flexibility of the proposed solution.

Sample calculations of the Neumann solution are done in Appendix E for a paraffin wax and the results plotted in figure 14, derived from figure 15, which shows a transition trace recorded on a continuous recorder for the transition of the first layer of the paraffin wax tests. Because of the infiniteness of the layer considered for the Neumann theoretical solution, the temperature gradients deviate as time proceeds away from the experimental plot representing a finite slab 3" thick.

2.3.2/.....

2.3.2 Numerical-relaxation Solution method.[7]

This solution is principally a finite interval numeric method and computations are done purely on an iteration basis (Appendix H). Consequently computerized calculations are essential to produce solutions of significance.

Although the same theoretical approach is utilised by Ständer and Lenhard [7] as in the method proposed in this work, the latter is an extension of the basic Schmidt method and is solvable graphically with reasonable accuracy. Transition is simply evaluated and results can be plotted in any form from the graphical or computed solutions with the approximate method proposed in this work.

The theory is symplified into three basic equations, one for the solid state, one for liquid state and the latter a transition heat balance. Solutions included by the authors[7] show that a decrease in finiteness, decreases the overall macroscopic error.

The evaluation of boundary conditions is not discussed in the work of Ständer and Lenhard[7].

3. Experimental.

As stated, the experimental work was performed to act as a basis of correlation for the formulated theory and solutions by alternative theories and to observe any characteristic phenomena during the conduction of the tests.

3.1/.....

3.1 Apparatus.

A model was constructed utilizing wax as the heat transfer material. The design considerations, construction of the model, auxiliary apparatus and experimental procedures are discussed in Appendix A and illustrated in the photographic plates 1 - 5.

3.2 Deductions.

The following deductions were made during the course of the experimental work.

(a) Heat flow was truly one dimensional.

(b) Convection was efficiently suppressed.

(c) Molten wax liberated air in the form of bubbles which accumulated on the heating plate.

(d) The defined step-heating was truly obtained and the heating plate showed only a slight drop in temperature for a small period (3° C for 2 minutes)

(e) A rapid rise in temperature was noted as the transition front passed the thermocouples - figure 11, 15, 16 and 21 and figures 4 and 20 in the printed experimental results.

3.3.1 Experimental Results.

The results of the experimental tests are shown in figures 4, 7A, 7B, 7C, 8, 9, 11, 14, 15, 16 and 19 for paraffin wax (P.W.)

as/.....

as the heat transfer material and figures 20 and 21 for beeswax (B.W.) as the heat transfer material.

The B.W. experimental test results are included for purposes of comparison (figures 20 and 21) since having a melting point of 61.5° C against the 51.5° C of the P.W, comparative calculations could not be done for the B.W. because of the unknown physical qualities of the compound.

The B.W. experimental results were discussed quantitively in the proceeding sections.

3.3.2 Graphical Solved Results.

The graphical computed results are shown in figures 5, 6, 7a, 8, 9, 10 and 13.

Figures 5 and 6 are the solution construction, figure 7 transition front travel/time and figure 8 - 13 heating curves for the devided layers.

3.3.3 Computed Results.

Computed results are shown in tables 1 - 7 and figures 7b, 7c, 7d, 8 and 12, where figures 7 represents transition front travel/time and figures 8 and 10 the heating curves.

4./.....

4. Conclusions:

From the foregoing discussion and analysis, it is clear that the approximate finite interval solution for transient heat conduction in a two-phase material with transition front shift, formulated in this work, produces rapid and accurate results. The accuracy depends upon whether the solutions are obtained graphically or computed numerically, and on the finiteness of the layers chosen.

Because of the capability of the method to handle any boundary condition in its application range, the method can be used to solve and optimise complex engineering problems with a high degree of accuracy. The solutions can be found graphically or numerically on a digital computer and can be plotted in any desired form.

The programmed solution used for the calculations in this work presents a great improvement on the graphical method of solution of solution on which it is based. Initial limitations to the program, due to insdequate dimensional storage of the computer memory, have been overcome by using refined programming. Thus the size of the program (Appendix I) does not present an obstacle to solution, even to a very high degree of accuracy or number of divisions.

Comparable analytical and numerical solutions, as referred to in the literature, cannot easily be applied to more complex and practical problems. The solutions obtained are limited to a classical nature, eg. HSU [1] and Carslaw and Jaeger [5] on the formation of ice on a water surface.

LITERATURE AND REFERENCES.

1. E.T. Eck - Engineering Heat Transfer - D. van Nostrand Company 1963.
2. W.H. Mc.Adams - Heat Transmission - McGraw-Hill Book Company, 1954.
3. W.E. Giedt - Principles of Engineering Heat Transfer - D. van Nostrand Company, 1957.
4. L. Grosse - Arbeitsmappe für Mineralölingenieure - V.D.I. Verlag, 1962.
5. H.S. Carslaw and J.C. Jaeger - Heat Conduction - Clarendon Press - 2nd Edition 1959.
6. L.L. van Zyl - An Electronic Analogue computer for the solution of non-linear partial differential equations encountered in the study of the self-heating of fishmeal - SACAC/SAROB Symposium No. 1 Johannesburg, September, 1963.
7. Wolfgang Stünder and Michael Lennard - Ebene Eindimensionale Wärmeleitprobleme bei Änderung des Aggregatzustands - V.D.I.-Z 108 (1966) Nr. 15 - Mai (III) p.667.
8. M. Abramowitz and I.E. Stegun - Handbook of Mathematical Functions - Government Printing Office, 1965.
9. M.N. Freed and C.J. Pallis - Analogue computer solutions of the Heat Conduction Equation - University of the Witwatersrand, Department of Mechanical Engineering, Report No. 18, July, 1963.
10. R.D. Zerkle and J.E. Sunderland - Journal of Heat Transfer, February, 1965.
11. H. Schlichting - Boundary layer Theory - Verlag G. Braun, 1951.

12./.....

12. R.S. Fairall - Unsteady-State Heat transfer in Solids with Radiation at one Boundary - Transaction ASME Journal of Heat Transfer - August 1962.
13. T.R. Goodman - The Heat-Balance Integral and Its Application to Problems Involving a Change of Phase - Transactions of the ASME Journal of Heat Transfer - February 1958.
14. H.G. Landau - Heat Conduction In a Melting Solid - Quarterly of Applied Mathematics, vol. 8 No. 1 - 1950.
15. C.A. Forster - Finite Difference Approach to Some Heat Conduction Problems Involving Changes of State -English Electric Company Ltd., Report L A.t. 059 - April 6 1954.

Computed Results : Table 1

15 Layers (17 divisions)

$dX = 0.3$ 6
$Z = 0.16$
$Z2 = 1.0$
$\Delta\tau = 2.54$ min
$\frac{\pi}{\varphi} = 70\ ^{\circ}C$

I.B.M. I620

k	TM	I+1										
T(0,I)	T(1,I)	T(2,I)	T(3,I)	....								
92.2	24.5	2										
93.3	51.5	24.5										
93.3	51.5	38.0	24.5									
93.6	51.5	43.0	36.7	30.4	27.8	25.3	24.9	24.5				
93.6	68.8	51.5	38.2	32.3	29.3	26.3	25.5	24.7	24.6	24.5		
93.7	72.5	51.5	41.9	33.7	29.3	27.4	25.5	25.0	24.6	24.5	24.	
5												
93.7	72.6	51.5	46.0	41.0	36.5	32.9	29.9	28.0	26.4	25.6	25.	
24.8	24.6	24.5	24.5	24.5								
93.7	72.6	59.3	46.2	41.2	36.9	33.2	30.4	28.2	26.8	25.7	25.	
2 24.8	24.6	24.5	24.5	24.5								
93.9	78.6	63.6	51.5	44.1	38.8	34.4	31.4	29.2	27.5	26.4	25.	
5 25.1	24.8	24.6	24.5	24.5								
94.0	79.6	65.6	51.5	46.3	41.6	37.4	33.9	31.2	29.1	27.6	26.	
5 25.8	25.2	25.0	24.8	24.7								
94.0	79.8	65.6	51.5	47.5	43.6	40.0	36.8	34.0	31.7	29.8	28.	
3 27.2	26.3	25.8	25.4	25.1								
94.0	79.8	65.6	56.5	47.5	43.7	40.2	37.0	34.2	31.9	30.0	28.	
5 27.3	26.5	25.8	25.4	25.2								
94.0	81.1	70.1	59.2	51.5	45.4	41.3	37.6	34.9	32.5	30.6	29.0	
27.8	26.9	26.2	25.7	25.3								
94.1	83.1	72.6	61.8	51.5	47.2	43.3	39.6	36.5	33.8	31.8	30.0	
26.7	27.6	26.8	26.2	25.7								
94.1	83.4	72.8	62.1	51.5	48.0	44.6	41.4	38.6	35.9	33.7	31.	
7 30.2	28.9	27.8	27.0	26.3								
94.1	83.4	72.8	62.1	51.5	48.3	45.2	42.3	39.5	37.0	34.8	32.	
8 31.1	29.7	28.5	27.6	26.8								
94.1	83.4	73.7	64.0	57.1	50.3	46.4	42.5	39.9	37.4	35.2	33.	
2 31.5	30.1	28.9	27.8	26.9								
94.1	83.9	73.7	65.4	57.1	51.5	46.4	43.1	40.0	37.5	35.3	33.	
4 31.6	30.2	28.9	27.9	27.0								
94.2	85.3	76.6	68.0	59.7	51.5	48.1	44.9	41.9	39.1	36.7	34.	
5 32.8	31.1	29.8	28.5	27.5								
94.2	85.6	77.0	68.5	60.0	51.5	48.5	45.7	43.0	40.4	38.0	35.	
8 33.9	32.2	30.6	29.2	28.0								
94.2	85.6	77.1	68.5	60.0	51.5	48.8	46.2	43.7	41.2	38.9	36.	
8 34.8	33.0	31.4	29.9	28.4								
94.2	85.6	77.1	68.5	60.0	54.4	48.8	46.2	43.7	41.3	39.0	36.	
9 34.9	33.1	31.4	29.9	28.5								
94.2	85.6	77.4	69.3	62.6	55.9	51.5	47.1	44.2	41.5	39.2	37.	
1 35.2	33.3	31.6	30.1	28.6								
94.2	86.2	78.8	71.2	64.5	57.8	51.5	48.3	45.4	42.5	40.0	37.	
7 35.6	33.7	32.0	30.3	28.8								
94.2	86.3	79.7	72.4	65.4	58.4	51.5	48.7	46.0	43.4	41.0	38.	
6 36.5	34.4	32.6	30.8	29.2								
94.2	87.0	79.9	72.7	65.6	58.5	51.5	48.9	46.4	43.9	41.6	39.	
3 37.1	35.1	33.7	31.3	29.5								
94.2	87.1	79.9	72.8	65.7	58.6	51.5	49.0	46.6	44.3	42.0	39.	
8 37.6	35.5	33.5	31.6	29.7								
94.2	87.1	79.9	72.8	65.7	58.6	53.8	49.0	46.7	44.3	42.0	39.	
8 37.6	35.6	33.6	31.6	29.8								
94.2	87.2	80.1	73.5	66.9	61.4	55.9	51.5	47.9	45.1	42.3	40.0	
37.8	35.7	33.7	31.8	29.9								

Computed Results : Table 2

15 Layers (15 divisions) $\Delta X = 0.3$
$Z' = 0.33\ (0.3 + 0.03)$
$Z2' = 1.0$
$\Delta\hat{T} = 2.54$ min
$\zeta_{\hat{T}}^{K} = 70\ ^{3}C$

I.B.M. 1620

k TM I+1

T(1,I) T(2,I) T(3,I) T(4,I) .....

1 16.7 2
51.5 24.5
2 .0 5
51.5 41.3 31.2 27.8 24.5
2 .0 7
79.5 51.5 34.6 30.4 26.1 25.3 24.5
2 48.9 12
82.5 51.5 44.0 36.6 32.3 27.9 26.5 25.0 24.8 24.5 24.5 24.5
3 .0 14
82.8 51.5 44.8 38.2 33.8 29.4 27.5 25.6 25.1 24.6 24.5 24.5 24.
5 .0 16
83.0 63.9 51.5 39.3 35.0 30.6 28.5 26.3 25.6 24.8 24.7 24.5 24.
24.5 24.5
3 22.6 22
84.5 68.0 51.5 45.2 40.0 34.8 31.7 28.6 27.2 25.8 25.3 24.8 24.
24.5 24.5
4 .0 31
84.5 68.0 51.5 46.9 42.4 38.6 34.9 32.3 29.7 28.2 26.7 26.0 25.
24.9 24.5
4 .0 32
84.5 68.0 57.5 46.9 42.8 38.6 35.5 32.3 30.2 28.2 27.1 26.1 25.
25.0 24.5
4 .0 35
86.5 73.2 60.8 51.5 44.6 40.3 36.0 33.4 30.8 29.1 27.5 26.7 25.
25.2

4 20.3 42
87.3 75.3 63.3 51.5 47.0 42.6 39.0 35.4 33.0 30.6 29.1 27
.7 26.8 26.1 25.7

4 59.6 52
87.3 75.3 63.4 51.5 47.8 44.2 41.0 37.8 35.3 32.8 31.1 29.4
28.2 27.2 26.5
5 .0 55
87.3 75.3 63.4 51.5 47.9 44.6 41.3 38.5 35.7 33.5 31.4 30.0
28.6 27.6 26.8
5 .0 59
87.8 76.6 67.1 57.9 51.5 46.0 42.3 39.0 36.3 34.2 32.1 30.5
29.1 28.0 27.1
5 3.8 62
88.4 78.3 68.5 59.9 51.5 47.3 43.3 39.9 37.0 34.6 32.7 30.9
29.5 28.3 27.3
5 29.9 72
88.8 79.4 70.0 60.7 51.5 48.1 44.8 41.8 39.0 36.4 34.2 32.3
30.7 29.2 28.0
5 50.7 82
88.8 79.5 70.1 60.8 51.5 48.5 45.6 42.8 40.2 37.7 35.5 33.5
31.7 30.1 28.6
6 .0 85
88.8 79.5 70.1 60.8 51.5 48.6 45.8 43.0 40.5 38.1 35.8 33.8
32.0 30.3 28.8
6 .0 89
89.0 79.9 71.0 63.6 56.3 51.5 46.8 43.7 40.8 38.4 36.2 34.2
32.3 30.6 29.0
6 2.5 92
89.2 80.5 72.5 64.7 58.1 51.5 47.9 44.4 41.5 38.7 36.5 34.4
32.5 30.8 29.1
6 21.4 102
89.7 81.9 74.1 66.4 58.9 51.5 48.5 45.5 42.7 40.1 37.7 35.4
33.3 31.4 29.6
6 44.9 112
89.8 82.1 74.4 66.7 59.1 51.5 48.7 46.0 43.4 40.8 38.4 36.1
34.0 31.9 30.0
6 69.8 122
89.8 82.2 74.5 66.8 59.1 51.5 48.9 46.3 43.8 41.3 39.0 36.7
34.5 32.3 30.3
7 .0 123
89.8 82.2 74.5 66.8 59.1 51.5 48.9 46.3 43.8 41.4 39.0 36.7
34.5 32.4 30.3
7 .0 128
89.9 82.4 75.2 68.1 62.2 56.3 51.5 47.7 44.7 41.7 39.3 36.9
34.7 32.6 30.4
7 2.5 132
90.1 82.8 75.7 69.2 62.8 57.1 51.5 48.2 45.1 42.3 39.5 37.1
34.8 32.6 30.5
7 17.1 142
90.4 83.6 77.0 70.4 64.0 57.7 51.5 48.6 45.7 43.0 40.3 37.6
35.4 33.1 30.8
7 35.0 152
90.5 83.9 77.3 70.8 64.3 57.9 51.5 48.7 46.0 43.4 40.8 38.3
35.8 33.4 31.1

Computed Results : Table 3.

15 Layers (15 divisions)

$\delta X = 0.3$
$Z = 0.46$ (0.3 + 0.16)
$Z2 = 1.0$
$\Delta\tau = 2.56$ min
$\frac{\sigma K}{\rho} = 70\ ^{\circ}C$

I.B.M. 1620

k TM I+1

T(1,I) T(2,I) T(3,I) T(4,I) .....

1	7.4	2									
51.5	24.3										
	2 .0	7									
51.5	43.0	34.6	30.4	26.1	25.3	24.5					
	2 .0	9									
73.1	51.5	36.7	32.3	27.8	26.3	24.9	24.7	24.5			
2	17.5	12									
76.4	51.5	48.5	35.6	31.5	27.4	26.2	25.0	24.8	24.5	24.5	24.5
3	.0	18									
77.6	51.5	45.6	39.8	35.6	31.3	29.1	26.8	25.9	25.1	24.8	24.6
24.5	24.5	24.5									
3	.0	22									
79.6	65.2	51.5	43.8	38.5	33.2	30.7	28.2	26.9	25.7	25.3	24.8
24.7	24.5	24.5									
3	.0	23									
79.7	65.5	51.5	45.0	38.5	34.6	30.7	28.8	26.9	26.1	25.3	25.0
24.7	24.5	24.6									
3	41.6	32									
79.8	65.6	51.5	46.7	42.4	38.1	34.9	31.7	29.8	27.9	26.9	25.9
25.5	25.1	24.9									
4	.0	38									
79.8	65.6	51.5	47.3	43.4	39.6	36.5	33.5	31.3	29.3	28.0	26.8
26.2	25.6	25.3									
4	.0	42									
82.1	70.2	59.5	51.5	45.2	41.0	37.4	34.4	32.2	30.1	28.7	27.4
26.7	26.0	25.6									
4	.8	43									
82.4	70.8	60.8	51.5	46.2	41.3	37.7	34.8	32.2	30.5	28.8	27.7
26.7	26.1	25.7									
5	26.5	52									
83.4	72.7	62.1	51.5	47.5	43.8	40.3	37.2	34.6	32.3	30.5	29.0
27.9	27.0	26.3									
5	61.6	62									
83.4	72.8	62.1	51.5	48.1	44.9	41.8	38.9	36.4	34.1	32.2	30.5
29.2	28.0	27.1									
5	.0	65									
83.4	72.8	62.1	51.5	48.2	45.1	42.1	39.4	36.8	34.6	32.6	31.0
29.5	28.3	27.3									
6	.0	69									
84.0	73.5	65.4	57.1	51.5	46.3	43.0	39.8	37.3	35.1	33.1	31.5
9.9	28.7	27.6									
5	.0	72									
84.8	75.6	66.7	59.0	51.5	47.6	43.8	40.7	37.8	35.5	33.5	31.8
30.3	28.9	27.8									
5	25.9	82									
85.5	76.0	68.4	59.9	51.5	48.3	45.2	42.3	39.5	37.1	34.9	33
31.2	29.7	28.3									
5	58.4	92									
85.6	77.1	68.5	60.0	51.5	48.6	45.8	43.2	40.6	38.2	36.0	34
32.1	30.4	28.9									
6	.0	98									
85.6	77.1	68.5	60.0	51.5	48.8	46.1	43.5	41.0	38.7	36.5	34
32.6	30.8	29.1									
6	.0	102									
85.6	77.4	69.3	62.6	55.0	51.4	47.0	44.1	41.3	39.0	36.8	34
32.8	31.0	29.3									
6	.0	104									
86.1	77.9	70.1	63.5	57.0	51.5	47.8	44.6	41.6	39.2	36.9	34
32.9	31.2	29.4									
6	11.9	112									
86.8	78.3	73.0	65.0	58.2	51.5	48.4	45.6	42.7	40.2	37.7	35
33.6	31.5	29.6									
6	33.1	122									
87.0	78.8	72.7	65.6	58.5	51.5	48.7	46.0	43.4	40.9	38.5	36
34.0	32.0	30.0									
6	54.5	132									
87.1	79.0	72.8	65.7	58.6	51.5	48.9	46.3	43.8	41.4	39.0	36
34.5	32.4	30.5									
7	.0	139									
87.1	79.0	72.8	65.7	58.6	51.5	48.9	46.5	44.0	41.6	39.3	37
34.7	32.8	30.5									
7	.0	142									
87.1	80.0	72.8	66.3	59.7	54.9	50.1	47.1	44.1	41.7	39.3	37
34.8	32.8	30.5									
7	.0	145									
87.2	80.1	72.5	66.9	61.3	55.8	51.5	47.7	44.8	41.9	39.5	37.
34.9	32.7	30.6									

Computed Results : Table 4A

30 Layers (32 divisions). $\Delta Z = 0.15$
$Z = 0.15$
$Z_0 = 1.0$
$\Delta t = 0.639$ min
$\frac{K}{C\gamma} = 70\ ^{\circ}C.$

I.B.M. 1620

k TM I+1

T(0,I) T(1,I) T(2,I) T(3,I) .....

3 .0 2
69.1 24.5

2 .0 3
77.2 46.8 24.5

2 .0 5
81.3 51.5 37.6 30.0 24.5

3 .0 13
83.3 51.5 44.7 38.1 33.5 29.3 27.2 25.5 25.0 24.6 24.5 24.
5

3 .0 13
83.4 64.0 44.8 39.1 33.7 30.3 27.4 26.1 25.0 24.7 24.5 24.
5 24.5

3 .0 14
83.5 64.1 51.5 39.2 34.7 30.5 28.2 26.2 25.4 24.8 24.6 24.
5 24.5 24.5

3 .0 22
85.0 68.2 51.5 45.7 40.7 35.5 32.5 29.4 27.7 26.2 25.5 25.0
24.7 24.6 24.5 24.5 24.5 24.5 24.5 24.5 24.5 24.5

4 .0 28
86.5 68.2 51.5 46.9 42.3 38.5 34.8 32.2 29.6 28.1 26.7 25.
9 25.3 25.0 24.7 24.6 24.5 24.5 24.5 24.5 24.5 24.5 24.5 24
.5 24.5 24.5 24.5 24.5 24.5

4 .0 32
86.5 71.8 60.7 50.1 44.6 39.1 35.9 32.8 30.7 28.6 27.4 26.
3 25.7 25.1 24.9 24.7 24.6 24.5 24.5 24.5 24.5 24.5 24.5 24
.5 24.5 24.5 24.5 24.5 24.5 24.5 24.5 24.5

4 .0 33
86.9 73.5 61.0 51.5 44.6 40.2 35.9 33.3 30.7 29.0 27.5 26.
5 25.7 25.3 24.9 24.7 24.6 24.5 24.5 24.5 24.5 24.5 24.5 24
.5 24.5 24.5 24.5 24.5 24.5 24.5 24.5 24.5

4 39.8 42
87.6 75.5 63.5 51.5 47.2 43.0 39.4 35.9 33.4 31.0 29.4 27.
8 26.9 26.1 25.6 25.2 24.9 24.7 24.6 24.5 24.5 24.5 24.5 24
.5 24.5 24.5 24.5 24.5 24.5 24.5 24.5 24.5

4 60.0 52
87.6 75.6 63.5 51.5 47.9 44.4 41.2 38.1 35.5 33.1 31.3 29.
5 28.3 27.2 26.5 25.8 25.5 25.1 24.9 24.7 24.6 24.5 24.5 24
.5 24.5 24.5 24.5 24.5 24.5 24.5 24.5 24.5

5 .0 52
87.6 75.6 63.5 51.5 47.9 44.5 41.2 38.4 35.6 33.4 31.3 29.
8 28.4 27.4 26.5 25.8 25.5 25.2 24.9 24.8 24.6 24.5 24.5 24
.5 24.5 24.5 24.5 24.5 24.5 24.5 24.5 24.5

5 .0 57
88.1 76.8 67.3 57.9 51.5 46.0 42.3 39.0 36.2 34.1 31.9 30.
4 28.9 27.9 26.9 26.3 25.7 25.4 25.1 24.9 24.7 24.6 24.6 24
.5 24.5 24.5 24.5 24.5 24.5 24.5 24.5 24.5 24.5

5 8.3 62
88.9 79.0 69.4 60.3 51.5 47.5 43.7 40.4 37.4 34.9 32.8 31.
0 29.7 28.4 27.5 26.7 26.1 25.6 25.3 25.0 24.9 24.7 24.6 24.
6 24.5 24.5 24.5 24.5 24.5 24.5 24.5 24.5

5 36.2 72
89.1 79.7 70.2 60.8 51.5 48.2 45.0 42.0 39.2 36.7 34.5 32.
5 31.0 29.5 28.5 27.5 26.8 26.2 25.8 25.4 25.2 24.9 24.8 24
.7 24.6 24.6 24.5 24.5 24.5 24.5 24.5 24.5

5 67.7 82
89.1 79.7 70.3 60.9 51.5 48.5 45.7 42.9 40.4 38.0 35.8 33.
9 32.2 30.7 29.5 28.4 27.6 26.9 26.3 25.9 25.5 25.2 25.0 24
.9 24.8 24.7 24.6 24.6 24.5 24.5 24.5 24.5

6 .0 83
89.1 79.7 70.3 60.9 51.5 48.6 45.7 43.0 40.5 38.1 35.9 34.
0 32.3 30.9 29.6 28.6 27.6 27.0 26.4 25.9 25.5 25.3 25.0 24.
9 24.8 24.7 24.6 24.6 24.5 24.5 24.5 24.5

6 .0 87
89.3 80.1 71.1 63.7 56.4 51.5 46.8 43.7 40.8 38.5 36.4 34.
5 32.7 31.3 30.0 28.9 28.0 27.3 26.6 26.1 25.7 25.4 25.2 25
.0 24.8 24.7 24.6 24.6 24.6 24.5 24.5 24.5

6 5.5 92
89.6 81.2 73.2 65.4 58.4 51.5 48.1 44.8 42.0 39.2 37.1 35.
0 33.3 31.7 30.5 29.3 28.4 27.6 26.9 26.4 25.9 25.6 25.3 25.
1 24.9 24.8 24.7 24.6 24.6 24.6 24.5 24.5

6 26.5 102
90.0 82.1 74.4 66.7 59.0 51.5 48.6 45.8 43.1 40.6 38.4 36.
2 34.5 32.8 31.4 30.2 29.2 28.2 27.5 26.9 26.4 26.0 25.6 25
.3 25.2 25.0 24.9 24.7 24.7 24.6 24.6 24.6

6 51.1 112
90.1 82.3 74.6 66.9 59.2 51.5 48.9 46.3 43.9 41.5 39.3 37.
3 35.5 33.8 32.4 31.0 30.0 28.9 28.2 27.4 26.9 26.4 26.0 25
.6 25.4 25.2 25.0 24.9 24.8 24.7 24.7 24.6

7 .0 120
90.1 82.3 74.6 66.9 59.2 51.5 49.0 46.6 44.3 42.0 40.0 38.
0 36.2 34.5 33.1 31.7 30.6 29.5 28.7 27.9 27.3 26.7 26.3 25.
9 25.6 25.4 25.2 25.0 24.9 24.8 24.8 24.7

7 .0 122
90.1 82.3 74.6 66.9 60.5 54.1 50.4 46.7 44.4 42.2 40.1 38.
1 36.4 34.7 33.2 31.8 30.7 29.6 28.8 28.0 27.4 26.8 26.4 26
.0 25.7 25.4 25.2 25.1 24.9 24.8 24.8 24.7

7 .0 126
90.1 82.5 75.4 68.2 62.3 56.5 51.5 48.1 45.3 42.6 40.5 38.
4 36.7 35.0 33.5 32.1 31.0 29.9 29.0 28.2 27.6 27.0 26.5 26
.1 25.8 25.5 25.3 25 . . . . . .

Computed Results : Table 4B

30 Layers (30 divisions) dX = 0.15
Z = 0.31 (.16 + .15)
Z2 = 1.15 (1 + .15)
$\Delta\tau$ = .635 min.
$\frac{K}{C_p}$ = 70 °C

I.B.M. 1620

k TM I

T(1,I) T(2,I) T(3,I) T(4,I) T(5,I) . . . . .

	1	61.8		2							
51.5	24.5										
	2	.0		3							
51.5	38.5	24.5									
	2	.0		5							
53.9	51.5	31.2	27.6	24.5							
	3	.0		10							
54.5	51.5	43.5	35.6	31.3	27.0	25.0	24.7	24.6	24.5		
	3	.0		12							
54.5	69.8	51.5	37.4	33.0	28.6	26.6	25.2	24.6	24.5	24	
.5	24.5										
	3	.0		22							
54.1	72.6	51.5	46.1	40.0	36.7	32.6	30.2	27.7	25.6	25	
.5	25.1	24.7	24.6	24.5	24.5	24.5	24.5	24.5	24.5	24.5	
24.5	24.5										
	4	.0		27							
54.2	78.9	68.6	51.5	46.8	39.0	34.2	31.6	29.0	27.6	26	
.2	25.6	25.0	24.8	24.5	24.5	24.5	24.5	24.5	24.5	24.5	
24.5	24.5	24.5	24.5	24.5	24.5						
	4	10.3		32							
54.2	79.9	69.7	51.5	46.2	41.1	37.2	33.3	31.0	28.7	27	
.4	25.2	25.7	25.1	24.9	24.7	24.5	24.5	24.5	24.5	24.5	
24.5	24.5	24.5	24.5	24.5	24.5	24.5	24.5	24.5	24.5		
	4	.0		43							
54.2	80.0	65.7	51.5	47.4	43.7	39.9	36.9	33.9	31.8	29	
.7	28.3	27.0	26.3	25.6	25.3	24.9	24.6	24.6	24.5	24.5	
24.5	24.5	24.5	24.5	24.5	24.5	24.5	24.5	24.5			
	5	.0		47							
54.2	81.3	70.2	59.3	51.5	45.4	41.3	37.7	34.8	32.6	30	
.8	29.0	27.6	26.8	25.0	25.6	25.1	24.9	24.7	24.6	24.5	
24.5	24.5	24.5	24.5	24.5	24.5	24.5	24.5	24.5	24.5		
	5	44.0		62							
54.3	83.6	72.8	62.7	51.5	47.9	44.5	41.3	38.3	35.7	33	
.3	31.5	30.0	28.6	27.6	26.7	26.2	25.6	25.3	25.0	24.8	
24.7	24.6	24.6	24.5	24.5	24.5	24.5	24.5	24.5	24.5		
	6	.0		78							
54.3	84.6	73.9	62.3	53.5	48.3	45.2	42.2	39.5	36.8	34	
.0	33.7	31.1	29.6	28.6	27.5	26.8	26.2	25.7	25.4	25.1	
24.9	24.8	24.7	24.6	24.5	24.5	24.5	24.5	24.5	24.5		
	6	.0		74							
54.3	84.6	73.9	65.5	57.2	51.5	46.4	43.1	40.0	37.5	35	
.3	33.3	31.6	30.1	29.0	27.9	27.1	26.4	26.3	25.5	25.3	
25.0	24.9	24.7	24.7	24.7	24.6	24.5	24.5	24.5	24.5		
	6	39.6		92							
54.3	85.7	77.1	68.5	65.0	51.5	48.5	45.6	42.9	40.3	37	
.6	35.0	33.9	32.2	30.0	29.6	28.6	27.7	27.1	26.5	26.0	
25.6	25.4	25.1	25.0	24.9	24.7	24.6	24.6	24.6			
	7	.0		108							
54.3	85.7	77.2	68.6	60.0	51.5	48.8	46.2	43.7	41.3	39	
.0	37.2	35.1	33.4	31.5	30.7	29.5	28.6	27.7	27.1	26.5	
26.1	25.7	25.5	25.2	25.0	24.9	24.8	24.7	24.6			

Computed Results : Table 5

30 Layers (32 divisions) dX = 0.15
Z = 0.16
Z2 = 1.0
$\Delta\tau$ = 0.635 min
$\frac{K}{C_p}$ = 126 °C

I.B.M. 1620

k TM I+1

T(0,I) T(1,I) T(2,I) T(3,I) . . . . . .

	2	.0		7					
51.5	43.5	34.6	30.4	26.1	25.3	24.5			
	2	.0		9					
80.6	51.5	36.7	32.3	27.8	26.3	24.9	24.7	24.5	
	2	69.4		17					
82.5	51.5	45.1	39.8	34.5	31.3	28.1	26.8	25.5	25.1
24.6	24.6	24.5	24.5	24.5	24.5				
	3	.0		20					
83.7	51.5	46.0	40.6	36.5	32.3	29.9	27.5	26.4	25.4
24.7	24.6	24.5	24.5	24.5	24.5	24.5	24.5	24.5	
	3	.0		22					
83.0	64.9	51.5	41.2	37.2	33.2	30.7	28.2	26.9	25.7
24.8	24.7	24.5	24.5	24.5	24.5	24.5	24.5	24.5	24.5
	3	50.1		32					
85.0	68.2	51.5	46.6	42.2	37.9	34.7	31.6	29.7	27.8
25.8	25.4	25.0	24.8	24.6	24.5	24.5	24.5	24.5	24.5
24.5	24.5	24.5	24.5	24.5	24.5	24.5	24.5	24.5	
	4	.0		45					
85.0	68.2	51.5	47.8	44.1	40.9	37.6	35.1	32.5	30.7
27.9	26.8	26.1	25.5	25.2	24.9	24.8	24.6	24.6	24.5
24.5	24.5	24.5	24.5	24.5	24.5	24.5	24.5	24.5	
	4	.0		47					
86.1	71.5	58.0	51.2	44.3	41.1	38.0	35.4	32.9	31.1
28.1	27.0	26.3	25.7	25.3	25.0	24.8	24.7	24.6	24.5
24.5	24.5	24.5	24.5	24.5	24.5	24.5	24.5	24.5	
	4	.0		49					
87.0	73.8	61.6	51.5	46.2	42.2	38.3	35.8	33.2	31.4
28.4	27.2	26.5	25.6	25.5	25.1	24.9	24.7	24.6	24.5
24.5	24.5	24.5	24.5	24.5	24.5	24.5	24.5	24.5	
	4	69.6		62					
87.6	75.6	63.5	51.5	48.0	44.6	41.5	38.5	36.0	33.6
30.1	29.0	27.8	27.0	26.3	25.8	25.4	25.2	24.9	24.8
24.6	24.5	24.5	24.5	24.5	24.5	24.5	24.5	24.5	
	4	116.2		77					
87.6	75.6	63.5	51.5	48.5	45.7	42.9	40.4	37.9	35.8
33.2	30.6	29.5	28.3	27.6	26.8	26.3	25.8	25.5	25.2
24.8	24.7	24.6	24.6	24.5	24.5	24.5	24.5	24.5	
	5	.0		80					
87.6	75.6	63.5	51.5	48.6	45.8	43.2	40.6	38.4	36.1
32.5	31.1	29.7	28.7	27.7	27.1	26.4	26.0	25.6	25.3
24.9	24.8	24.7	24.6	24.6	24.5	24.5	24.5	24.5	
	5	.0		84					
88.1	76.9	67.6	58.4	51.5	47.2	44.1	41.0	38.7	36.5
32.9	31.5	30.1	29.1	28.0	27.3	26.6	26.2	25.7	25.4
25.0	24.8	24.7	24.6	24.6	24.5	24.5	24.5	24.5	
	5	19.6		92					
89.0	79.4	70.0	60.6	51.5	48.3	45.4	42.4	40.0	37.6
33.7	32.3	30.8	29.7	28.7	27.9	27.1	26.6	26.1	25.7
25.2	25.0	24.9	24.7	24.7	24.6	24.6	24.5	24.5	

5 66.9 107
89.1 79.7 70.3 60.9 51.5 48.9 46.3 43.9 41.4 39.3 37.2
35.4 33.7 32.3 31.0 29.9 28.9 28.1 27.4 26.8 26.3 26.0 25
.6 25.4 25.1 25.0 24.9 24.8 24.7 24.6 24.6 24.6
5 120.6 122
89.1 79.7 70.3 60.9 51.5 49.1 46.8 44.6 42.4 40.3 38.5
36.6 35.1 33.5 32.2 31.0 30.0 29.0 28.3 27.5 27.0 26.5 26
.1 25.8 25.5 25.3 25.1 25.0 24.9 24.8 24.7 24.7
6 .0 124
89.1 79.7 70.3 60.9 51.5 49.1 46.9 44.6 42.6 40.5 38.6
36.8 35.2 33.6 32.4 31.1 30.1 29.1 28.4 27.7 27.1 26.6 26
.2 25.8 25.6 25.3 25.2 25.0 24.9 24.8 24.7 24.7
6 .0 128
89.1 80.1 71.2 64.0 56.3 51.5 47.9 46.2 42.8 40.7 38.9
37.9 36.5 35.0 33.7 31.4 30.4 29.4 28.6 27.9 27.3 26.7 26
.3 25.9 25.7 25.4 25.2 25.1 24.9 24.8 24.8 24.7
6 16.7 137
89.1 80.8 74.0 66.2 58.8 51.5 48.9 46.3 43.9 41.7 39.7
37.8 36.1 34.6 33.2 32.0 30.9 30.0 29.1 28.4 27.7 27.1 26
.6 26.3 25.9 25.7 25.4 25.2 25.1 25.0 24.9 24.8
6 35.5 152
89.1 80.3 74.6 66.9 59.1 51.5 48.2 47.0 44.6 42.6 40.8
39.0 37.5 36.7 34.3 33.0 31.9 30.8 29.9 29.1 28.4 27.7 27
.2 26.7 26.4 26.0 25.8 25.5 25.3 25.2 25.1 25.0
6 37.8 167
89.1 80.3 74.6 66.9 59.2 51.5 48.4 47.4 45.4 43.5 41.8
40.1 38.6 36.7 35.2 34.0 32.7 31.7 30.7 29.8 29.0 28.3 27
.4 27.0 26.8 26.5 26.1 25.9 25.6 25.5 25.3 25.2
7 .0 178
89.1 80.3 74.6 66.9 59.2 51.5 49.5 47.6 45.7 43.8 42.1
40.4 38.9 37.3 35.9 34.5 33.2 32.2 31.3 30.3 29.6 28.9 28
.2 27.7 27.2 26.8 26.4 26.1 25.9 25.6 25.5 25.3

Computed Results : Table 6

30 Layers (32 divisions)

dX = 0.15
Z = 0.16
Z2 = 1.0
$\Delta\hat{t}$ = 0.635 min
$\frac{M}{C_f}$ = 98 lbs.

I.B.M. 1620

k TM I+1

T(0,I) T(1,I) T(2,I) T(3,I) .....

2 .0 6
51.5 41.3 34.6 27.8 26.1 24.5
2 .0 8
80.3 51.5 36.7 30.4 27.8 25.3 24.9 24.5
2 35.8 12
88.0 51.5 43.5 36.6 31.5 27.9 26.2 25.0 24.8 24.5 24.5
2 .0 17
88.5 51.5 45.4 39.8 35.0 31.3 28.5 26.8 25.6 25.1 24.7 24
24.5 24.5 24.5 24.5 24.5
2 .0 19
88.7 64.6 51.5 40.6 35.9 32.3 29.4 27.5 26.1 25.4 24.8 24
24.5 24.5 24.5 24.5 24.5 24.5 24.5
3 9.9 22
88.8 68.2 51.5 44.8 38.6 34.2 30.7 28.4 26.9 25.8 25.3 24
24.7 24.5 24.5 24.5 24.5 24.5 24.5 24.5 24.5 24.5
3 65.8 32
85.0 68.2 51.5 46.8 42.4 38.4 34.9 32.1 29.8 28.1 26.9
26.0 25.4 25.0 24.8 24.6 24.6 24.5 24.5 24.5 24.5 24.5 24
.5 24.5 24.5 24.5 24.5 24.5 24.5 24.5 24.5 24.5 24.5
4 .0 38
85.0 68.2 51.5 47.4 43.4 39.8 36.5 33.7 31.3 29.4 28.0
26.9 26.1 25.5 25.1 24.8 24.7 24.6 24.5 24.5 24.5 24.5 24
.5 24.5 24.5 24.5 24.5 24.5 24.5 24.5 24.5 24.5 24.5
4 .0 42
86.9 73.7 61.4 51.5 45.6 41.3 37.4 34.6 32.2 30.3 28.7
27.5 26.6 25.9 25.4 25.0 24.8 24.7 24.6 24.5 24.5 24.5 24
.5 24.5 24.5 24.5 24.5 24.5 24.5 24.5 24.5 24.5 24.5
4 2.0 43
87.1 74.2 62.6 51.5 46.4 41.5 38.0 34.8 32.4 30.5 28.9
27.6 26.7 26.0 25.4 25.1 24.9 24.7 24.6 24.5 24.5 24.5 24
.5 24.5 24.5 24.5 24.5 24.5 24.5 24.5 24.5 24.5 24.5
4 34.9 52
87.6 75.5 63.5 51.5 47.5 43.8 40.3 37.3 34.5 32.3 30.4
28.9 27.5 26.9 26.2 25.7 25.3 25.0 24.8 24.7 24.6 24.5 24
.5 24.5 24.5 24.5 24.5 24.5 24.5 24.5 24.5 24.5 24.5
4 77.1 62
87.6 75.6 63.5 51.5 48.1 44.9 41.8 39.0 36.4 34.1 32.1
30.5 29.1 28.0 27.1 26.4 25.9 25.5 25.2 24.9 24.8 24.7 24
.6 24.5 24.5 24.5 24.5 24.5 24.5 24.5 24.5 24.5 24.5
5 .0 67
87.6 75.6 63.5 51.5 48.3 45.3 42.4 39.6 37.1 34.8 32.9
31.2 29.8 28.6 27.6 26.8 26.2 25.7 25.4 25.1 24.9 24.8 24
.7 24.6 24.5 24.5 24.5 24.5 24.5 24.5 24.5 24.5 24.5
5 .0 71
88.1 76.9 67.4 58.2 51.5 46.6 43.3 40.0 37.6 35.4 33.4
31.7 30.2 28.9 28.0 27.2 26.5 26.0 25.6 25.3 25.0 24.9 24
.7 24.6 24.6 24.5 24.5 24.5 24.5 24.5 24.5 24.5 24.5

```
                5          9          12
  88.4  77.8  67.5  59.4  51.5  47.4  43.3  40.4  37.7  35.5  33.5
31.6  30.3  29.1  28.1  27.2  26.6  26.0  25.6  25.3  25.1  24.9  24
.8  24.7  24.6  24.5  24.5  24.5  24.5  24.5  24.5  24.5  24.5
                5         26.8        82
  89.1  79.6  70.1  60.8  51.5  46.3  45.1  42.2  39.5  37.1  34.9
33.1  31.5  30.2  29.0  28.1  27.3  26.6  26.1  25.7  25.4  25.1  25
.0  24.8  24.7  24.6  24.6  24.5  24.5  24.5  24.5  24.5
                5         58.5        92
  89.1  79.7  70.3  60.9  51.5  48.6  45.8  43.2  40.6  38.4  36.2
34.3  32.6  31.2  30.0  29.0  28.0  27.3  26.7  26.2  25.8  25.5  25
.2  25.0  24.8  24.8  24.7  24.6  24.6  24.5  24.5  24.5
                5         92.1       102
  89.1  79.7  70.3  60.9  51.5  48.9  46.3  43.9  41.5  39.3  37.2
35.4  33.7  32.2  30.9  29.7  28.8  27.9  27.2  26.7  26.2  25.8  25
.5  25.3  25.1  24.9  24.8  24.7  24.6  24.6  24.6  24.6
                6          0         104
  89.1  79.7  70.3  60.9  51.5  48.9  46.4  44.0  41.6  39.5  37.4
35.6  33.9  32.4  31.0  29.8  28.9  28.1  27.4  26.8  26.3  25.9  25
.6  25.3  25.1  24.9  24.8  24.7  24.7  24.6  24.5  24.5
                6          9         108
  89.3  80.1  71.1  63.9  56.6  51.5  47.4  44.6  41.9  39.8  37.7
35.9  34.2  32.7  31.4  30.2  29.2  28.3  27.6  27.0  26.5  26.0  25
.7  25.4  25.2  25.0  24.9  24.8  24.7  24.7  24.6  24.6
                6         5.1        112
  89.6  80.1  72.0  65.4  58.2  51.5  48.3  45.4  42.6  40.3  38.1
36.2  34.5  33.1  31.7  30.5  29.5  28.6  27.8  27.2  26.6  26.2  25
.8  25.5  25.3  25.1  25.0  24.8  24.8  24.7  24.5  24.5
                6         26.9        122
  89.8  82.4  74.3  66.6  59.0  51.5  48.8  46.2  43.7  41.4  39.2
37.2  35.5  33.9  32.5  31.3  30.2  29.2  28.4  27.7  27.1  26.6  26
.2  25.8  25.6  25.3  25.1  25.0  24.9  24.8  24.7  24.7
                6         52.2        132
  90.1  82.3  74.6  66.9  59.1  51.5  49.0  46.7  44.3  42.2  40.1
38.2  36.4  34.8  33.3  32.0  30.9  29.9  29.0  28.3  27.6  27.0  26
.6  26.2  25.8  25.6  25.3  25.2  25.0  24.9  24.9  24.8
                6         79.3        142
  90.1  82.3  74.6  66.9  59.2  51.5  49.2  47.0  44.8  42.7  40.7
38.8  37.1  35.5  34.1  32.8  31.6  30.5  29.6  28.8  28.1  27.5  26
.9  26.5  26.1  25.8  25.6  25.4  25.2  25.1  25.0  24.9
```

Computed Results : Table 7

5 Layers (5 divisions)

$\Delta x = 0.5$
$Z = 1.06\ (0.9 + 0.1\varepsilon)$
$Z2 = 1.9\ (1.0 + 0.9)$
$\Delta\tau = 22.82$ min
$\frac{k}{C\rho} = 70$ °C.

I.B.M. 1620

k	TM	I+1		
T(1,I)	T(2,I)	T(3,I)	T(4,I)	T(5,I)
2	.0	5		
51.5	41.3	31.2	27.8	26.5
2	.0	7		
78.0	51.5	35.1	30.9	28.4
2	48.2	12		
81.6	51.5	44.5	38.2	32.9
3	.0	15		
81.9	51.5	45.2	39.3	33.6
3	.0	17		
82.0	63.7	51.5	39.5	33.7
3	15.3	22		
83.6	67.5	51.5	44.0	36.5
3	58.7	32		
83.6	67.5	51.5	44.0	36.5
4	.0	35		
83.6	67.5	51.5	44.0	36.5
4	.0	42		
85.7	72.9	61.0	50.1	40.3
4	.0	46		
86.3	74.3	62.7	51.5	41.3
4	4.8	52		
86.5	74.6	63.1	51.5	41.7
4	14.5	62		
86.5	74.6	63.1	51.5	41.7
4	24.3	72		
86.5	74.8	63.1	51.5	41.7
4	34.0	82		
86.5	74.8	63.1	51.5	41.7
4	43.8	92		
86.5	74.8	63.1	51.5	41.7
4	53.6	102		
86.5	74.8	63.1	51.5	41.7
4	63.4	112		
86.5	74.8	63.1	51.5	41.7
5	.0	119		
86.5	74.8	63.1	51.5	41.7
5	.0	122		
86.6	75.1	63.5	52.7	41.9
5	.0	132		
86.8	75.6	64.5	53.3	42.3
5	.0	142		
86.9	75.7	64.6	53.5	42.4
5	.0	152		
86.9	75.8	64.6	53.5	42.4
5	.0	162		
86.9	75.8	64.6	53.5	42.4

Table 8:
Summed time intervals tabulated.

i+1	i	$\Delta\tau$=22.82	$\Delta\tau$=2.54	$\Delta\tau$=.635	(min.)
2	1	22.82	2.54	.635	
3	2	45.64	5.08	1.27	
4	3	68.46	7.62	1.90	
5	4	91.28	10.16	2.54	
6	5	114.10	12.70	3.17	
7	6	136.92	15.24	3.81	
8	7	159.74	17.78	4.44	
9	8	182.56	20.32	5.08	
10	9	205.38	22.86	5.71	
11	10	228.20	25.40	6.35	
12	11	251.02	27.94	6.98	
13	12	273.84	30.48	7.62	
14	13	296.66	33.02	8.25	
15	14	319.48	35.56	8.89	
16	15	342.30	38.10	9.52	
17	16	365.12	40.64	10.16	
18	17	387.94	43.18	10.79	
19	18	410.76	45.72	11.43	
20	19	433.58	48.26	12.06	
21	20	456.40	50.80	12.70	
22	21	479.22	53.34	13.33	
23	22	502.04	55.88	13.97	
24	23	524.86	58.42	14.60	
25	24	547.68	60.96	15.24	
26	25	570.50	63.50	15.87	
27	26	593.32	66.04	16.51	
28	27	616.14	68.58	17.14	
29	28	638.96	71.12	17.78	
30	29	661.78	73.66	18.41	
31	30	684.60	76.20	19.05	
32	31	707.42	78.74	19.68	
33	32	730.24	81.28	20.32	
34	33	753.06	83.82	20.95	
35	34	775.88	86.36	21.59	
36	35	798.70	88.90	22.22	
37	36	821.52	91.44	22.86	
38	37	844.34	93.98	23.49	
39	38	867.16	96.52	24.13	
40	39	889.98	99.06	24.76	
41	40	912.80	101.60	25.40	
42	41	935.62	104.14	26.02	
43	42	958.44	106.68	26.67	
44	43	981.26	109.22	27.30	
45	44	1004.08	111.76	27.94	
46	45	1026.90	114.30	28.57	
47	46	1049.72	116.84	29.21	
48	47	1072.54	119.38	29.84	
49	48	1095.36	121.92	30.48	
50	49	1118.18	124.46	31.11	
51	50	1141.00	127.00	31.75	
52	51	1163.82	129.54	32.38	
53	52	1186.64	132.08	33.02	
54	53	1209.46	134.62	33.65	
55	54	1232.28	137.16	34.29	
56	55	1255.10	139.70	34.92	
57	56	1277.92	142.24	35.56	
58	57	1300.74	144.78	36.19	
59	58	1323.56	147.32	36.83	
60	59	1346.38	149.86	37.46	
61	60	1369.20	152.40	38.10	
62	61	1392.02	154.94	38.73	
63	62	1414.84	157.48	39.37	
64	63	1437.66	160.02	40.00	
65	64	1460.48	162.56	40.64	
66	65	1483.30	165.10	41.27	
67	66	1506.12	167.64	41.91	
68	67	1528.94	170.18	42.54	
69	68	1551.76	172.72	43.18	
70	69	1574.58	175.26	43.81	
71	70	1597.40	177.80	44.45	
72	71	1620.22	180.34	45.09	
73	72	1643.04	182.88	45.72	
74	73	1665.86	185.42	46.35	
75	74	1688.68	187.96	46.99	
76	75	1711.50	190.50	47.62	
77	76	1734.32	193.04	48.26	
78	77	1757.14	195.58	48.89	
79	78	1779.96	198.12	49.53	
80	79	1802.78	200.66	50.16	
81	80	1825.60	203.20	50.80	
82	81	1848.42	205.74	51.43	
83	82	1871.24	208.28	52.07	
84	83	1894.06	210.82	52.70	
85	84	1916.88	213.36	53.34	
86	85	1939.70	215.90	53.97	
87	86	1962.52	218.44	54.61	
88	87	1985.34	220.98	55.24	
89	88	2008.16	223.52	55.88	
90	89	2030.98	226.06	56.51	
91	90	2053.80	228.60	57.15	
92	91	2076.62	231.14	57.78	
93	92	2099.44	233.68	58.42	
94	93	2122.26	236.22	59.05	
95	94	2145.08	238.76	59.69	
96	95	2167.90	241.30	60.32	
97	96	2190.72	243.84	60.96	
98	97	2213.54	246.38	61.59	
99	98	2236.36	248.92	62.23	
100	99	2259.18	251.46	62.86	
101	100	2282.00	254.00	63.50	
102	101	2304.82	256.54	64.13	
103	102	2327.64	259.08	64.77	
104	103	2350.46	261.62	65.40	
105	104	2373.28	264.16	66.04	
106	105	2396.10	266.70	66.67	
107	106	2418.92	269.24	67.31	
108	107	2441.74	271.78	67.94	
109	108	2464.56	274.32	68.58	
110	109	2487.38	276.86	69.21	
111	110	2510.20	279.40	69.85	
112	111	2533.02	281.94	70.48	
113	112	2555.84	284.48	71.12	
114	113	2578.66	287.02	71.75	
115	114	2601.48	289.56	72.39	
116	115	2624.30	292.10	73.02	
117	116	2647.12	294.64	73.66	

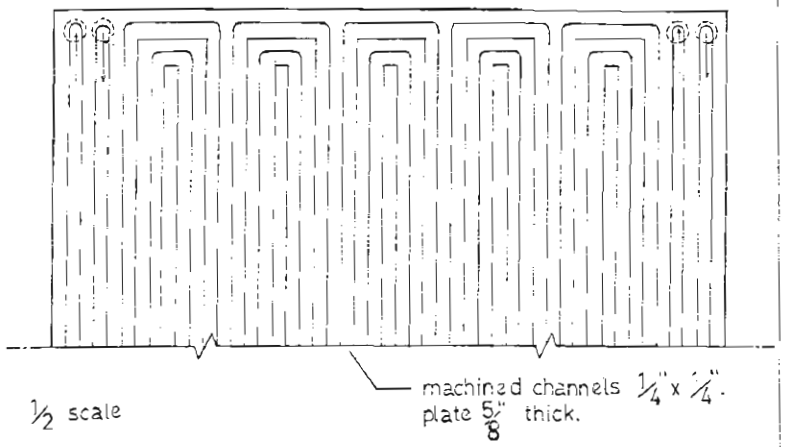

Copper heat/cooling mode.

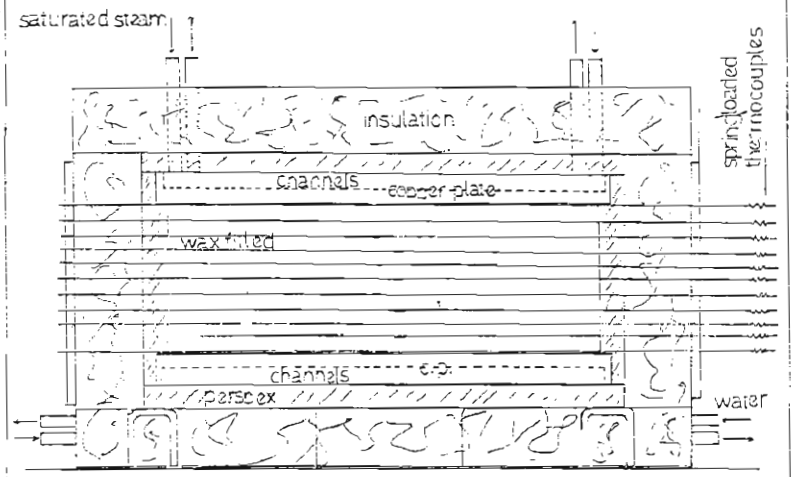

Layout of experimental apparatus.

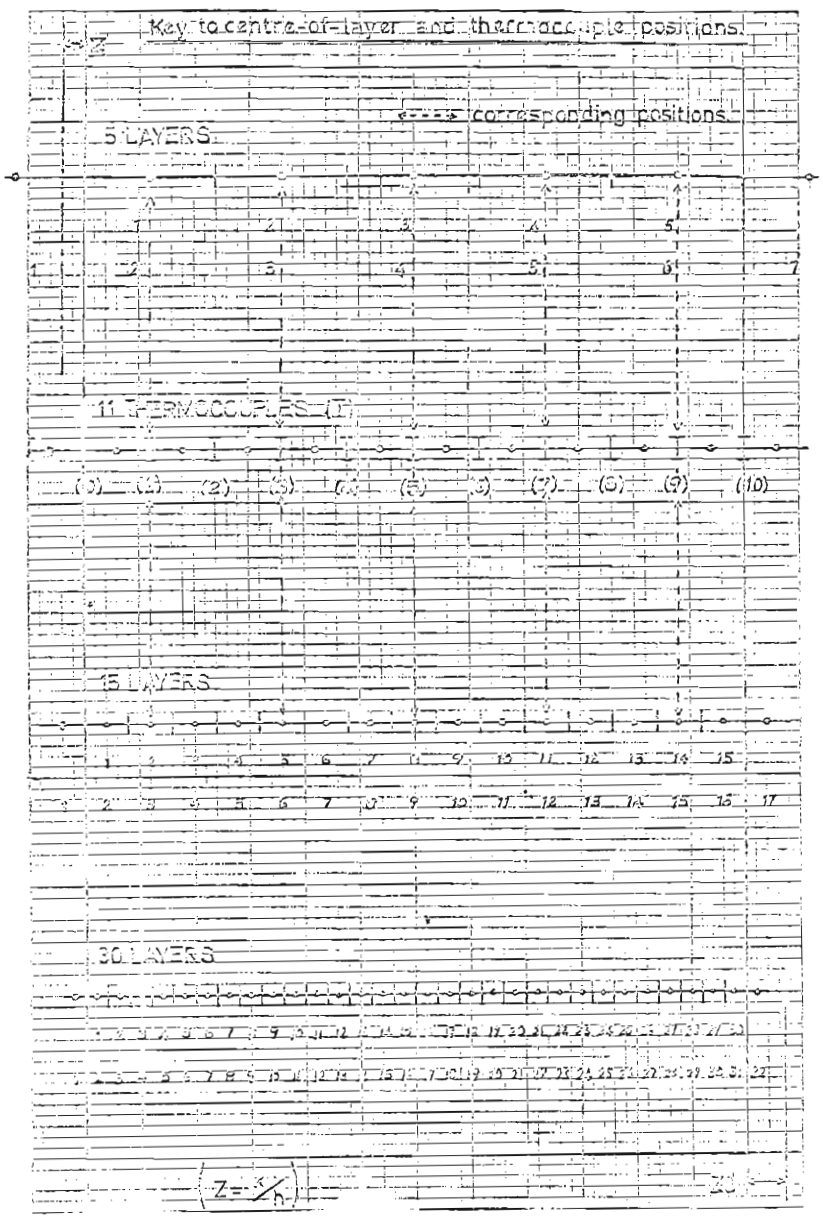
Key to centre-of-layer and thermocouple positions.
corresponding positions.
5 LAYERS
11 THERMOCOUPLES (T)
15 LAYERS
30 LAYERS
(Z = x/h)

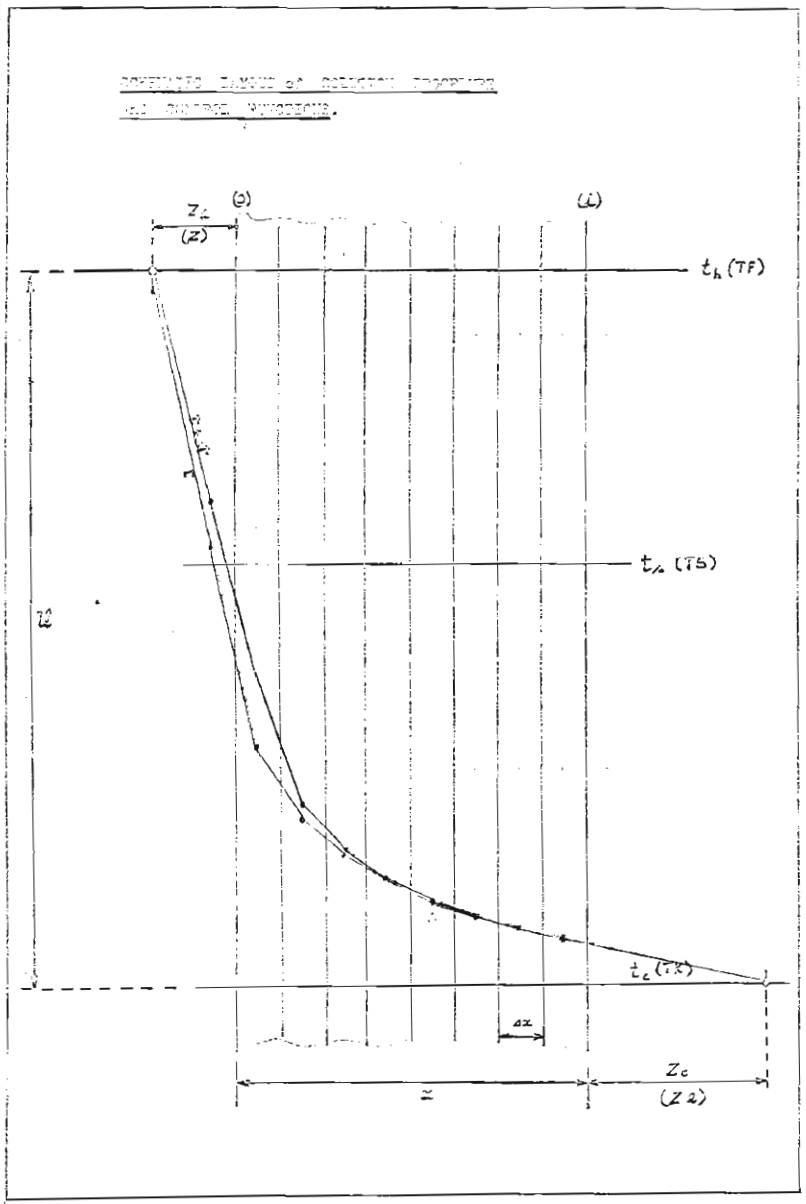
(0)
(1)
Z_c
(Z)
t_h (TF)
t_s (TS)
t_c (TC)
Δx
Z
Z_c
(Z2)

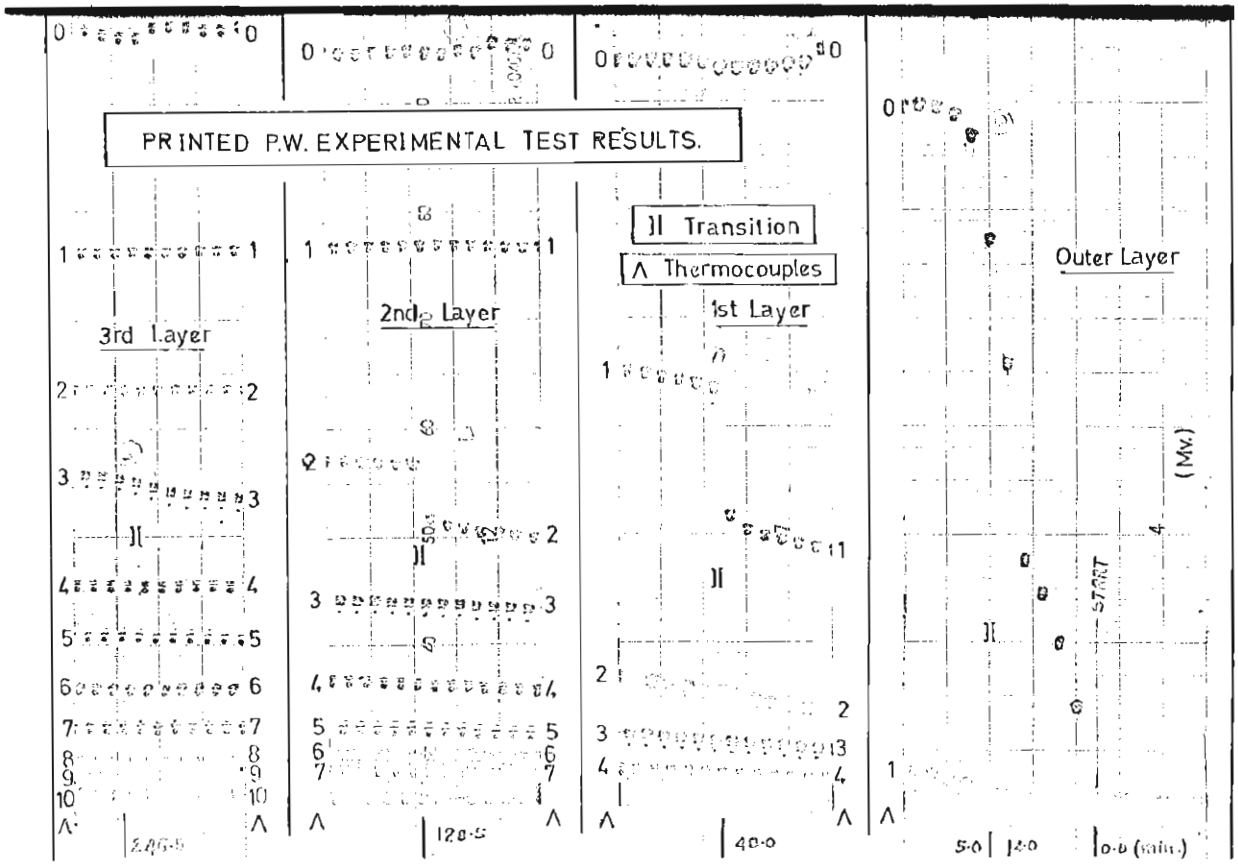
PRINTED P.W. EXPERIMENTAL TEST RESULTS.
Transition
Thermocouples
3rd Layer
2nd Layer
1st Layer
Outer Layer
START
(Mv.)
240·0
120·5
40·0
5·0
1·0
0·0 (min.)

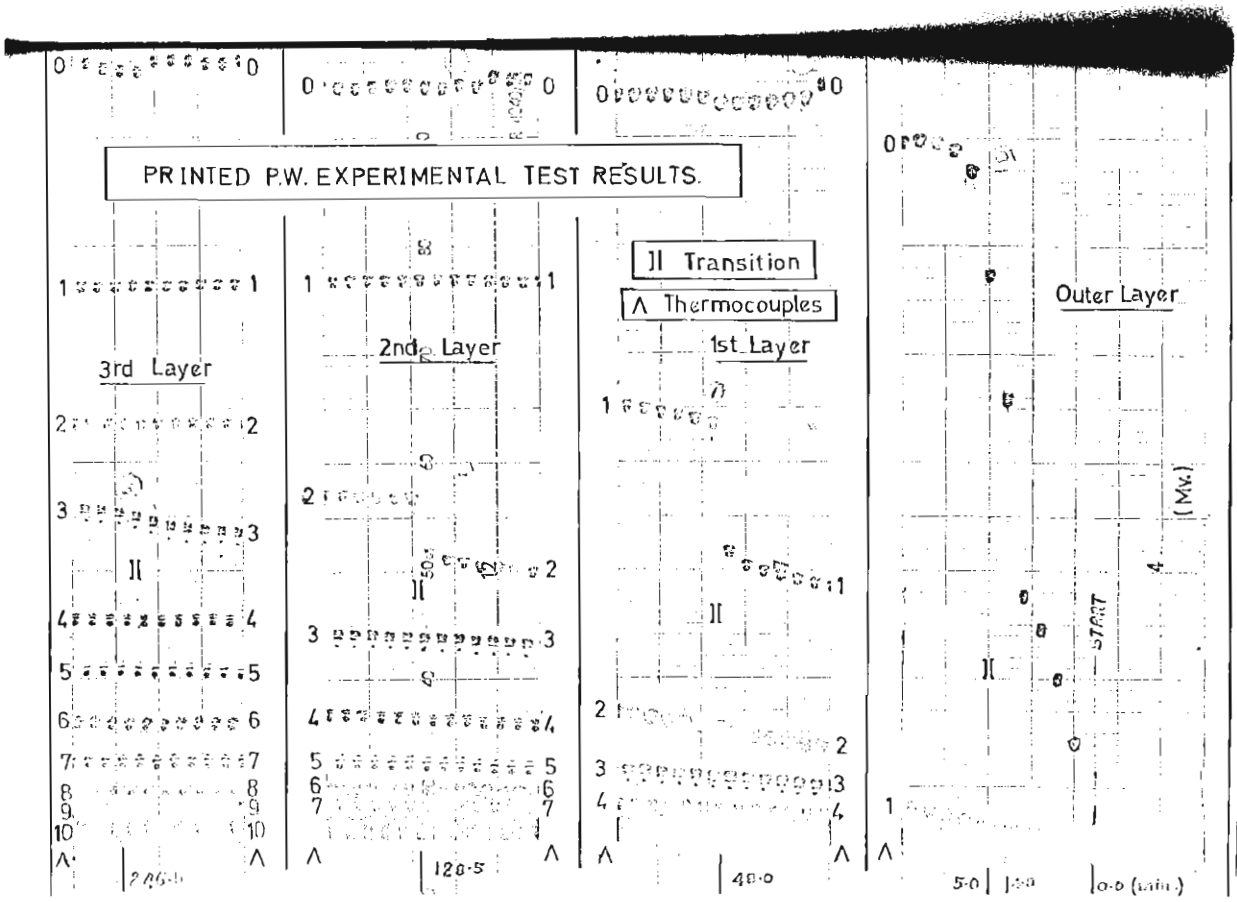
PRINTED P.W. EXPERIMENTAL TEST RESULTS.
Transition
Thermocouples
3rd Layer
2nd Layer
1st Layer
Outer Layer
START
(Mv.)
240·0
120·5
40·0
5·0
1·0
0·0 (min.)

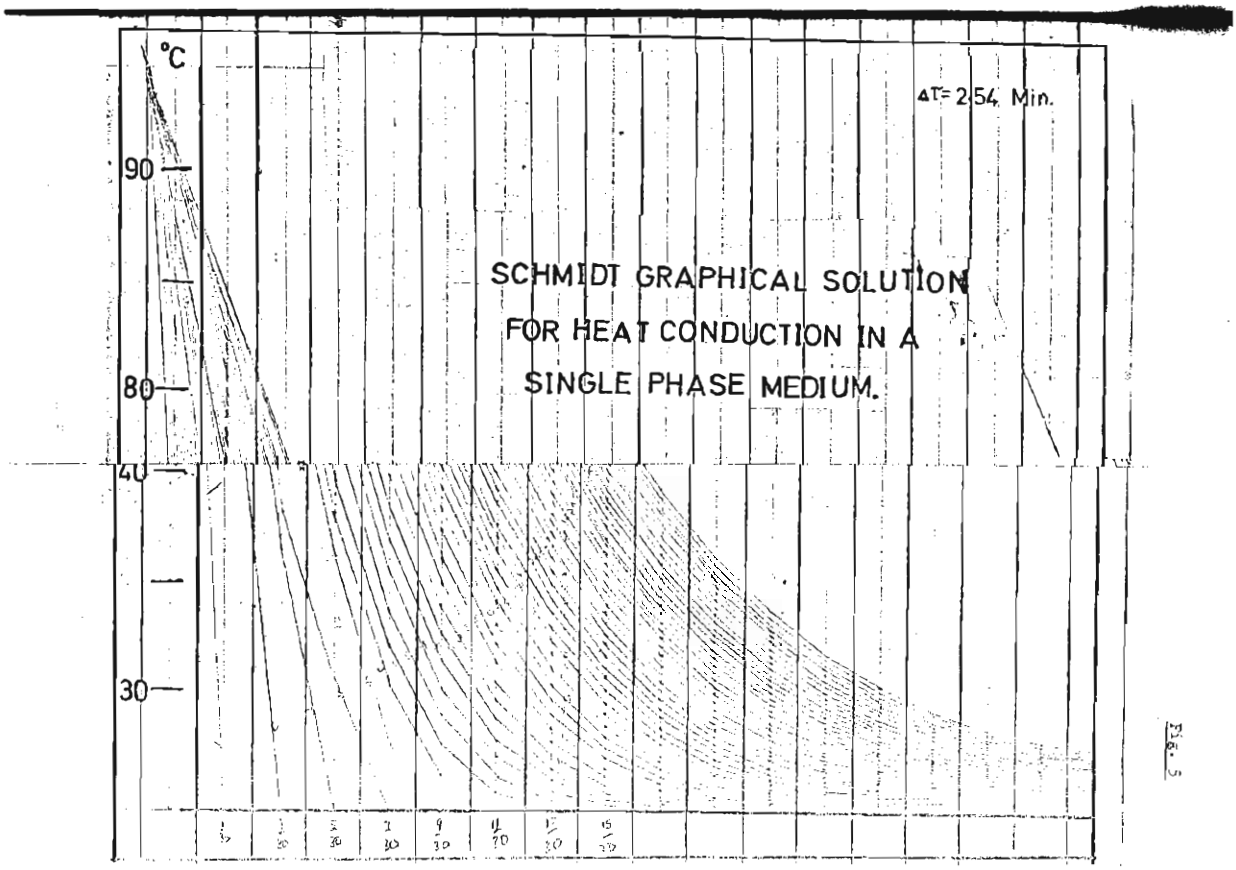
°C
90
80
40
30
ΔT= 2.54 Min.
SCHMIDT GRAPHICAL SOLUTION
FOR HEAT CONDUCTION IN A
SINGLE PHASE MEDIUM.

Fig. 5

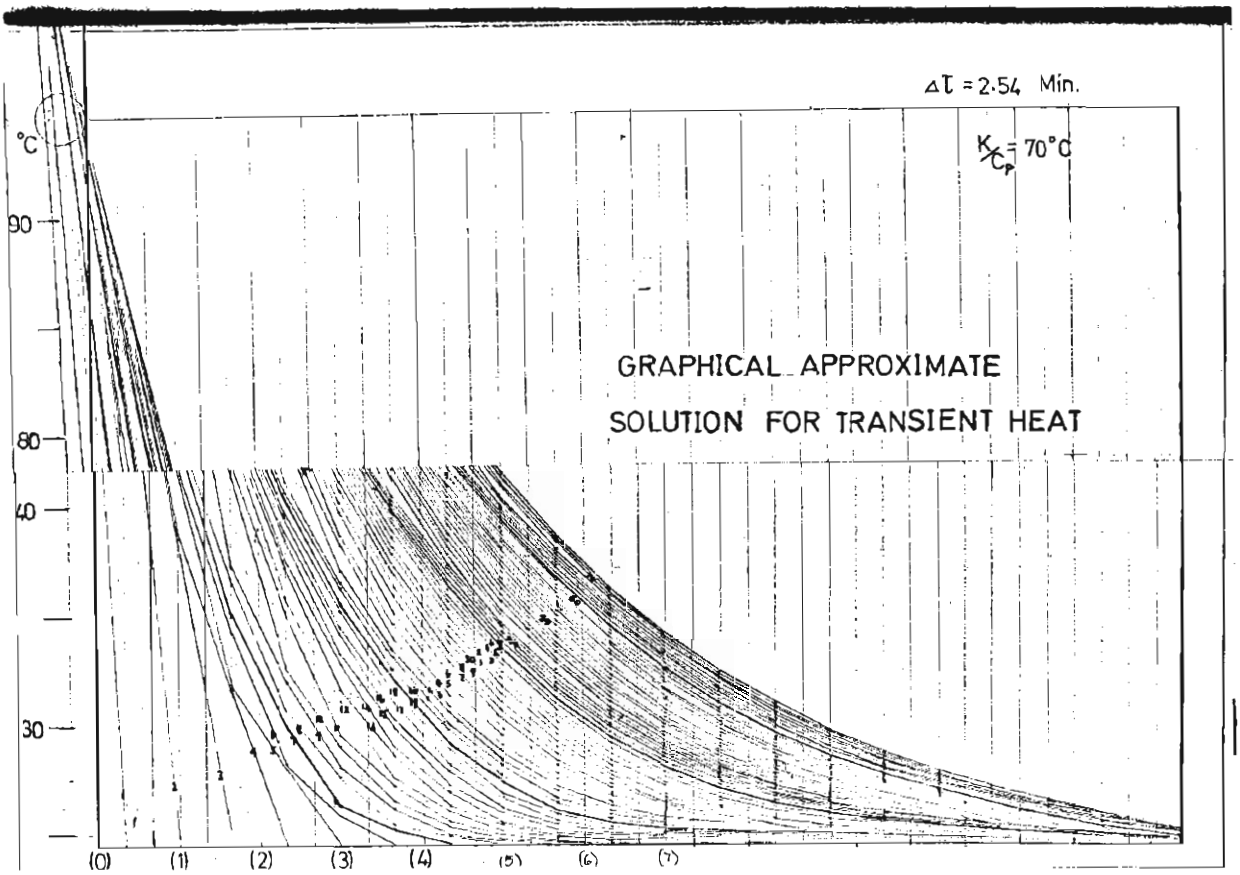
°C
90
80
40
30
Δτ = 2.54 Min.
K/C_r = 70°C
GRAPHICAL APPROXIMATE
SOLUTION FOR TRANSIENT HEAT
(0)
(1)
(2)
(3)
(4)
(5)
(6)
(7)

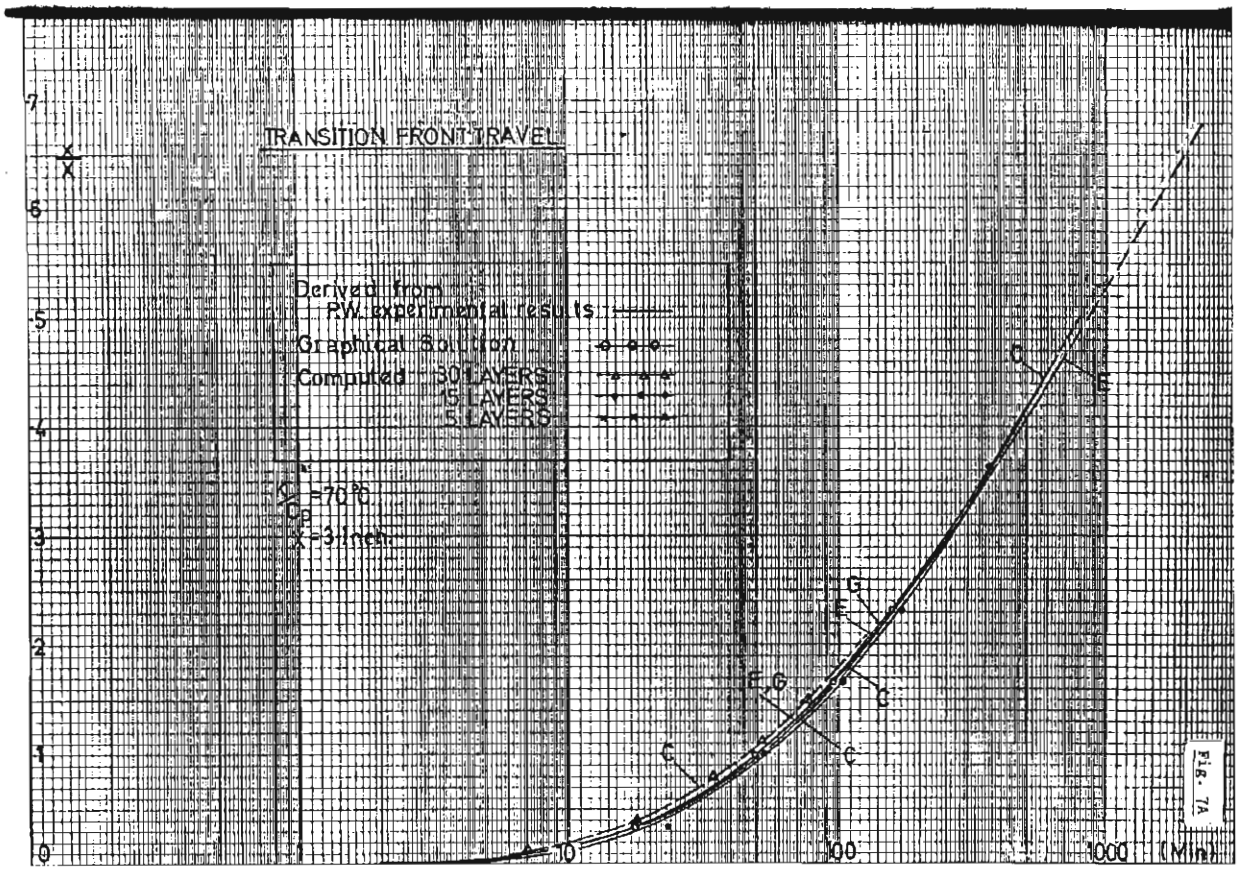
TRANSITION FRONT TRAVEL
X/X
Derived from
R.W. experimental results
Graphical Solution
Computed - 30 LAYERS
15 LAYERS
5 LAYERS
K/Cp = 70 °C
X = 3 Inch
C
E
G
0
1
2
3
4
5
6
7
10
100
1000 (Min)

Fig. 7A

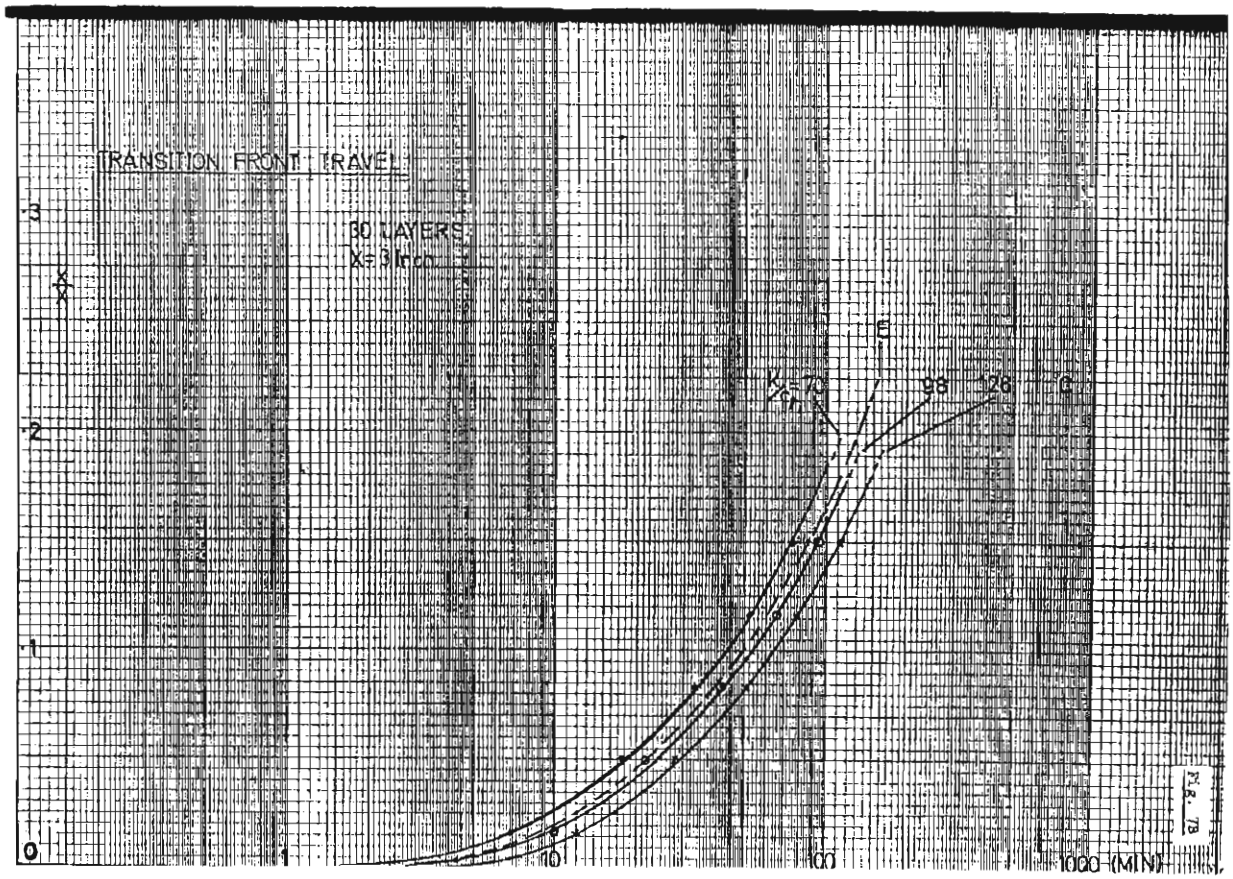
TRANSITION FRONT TRAVEL
30 LAYERS
X = 3 Inch
X/X
K/Cp = 70
98
126
E
G
0
1
2
3
10
100
1000 (MIN)

Fig. 7B

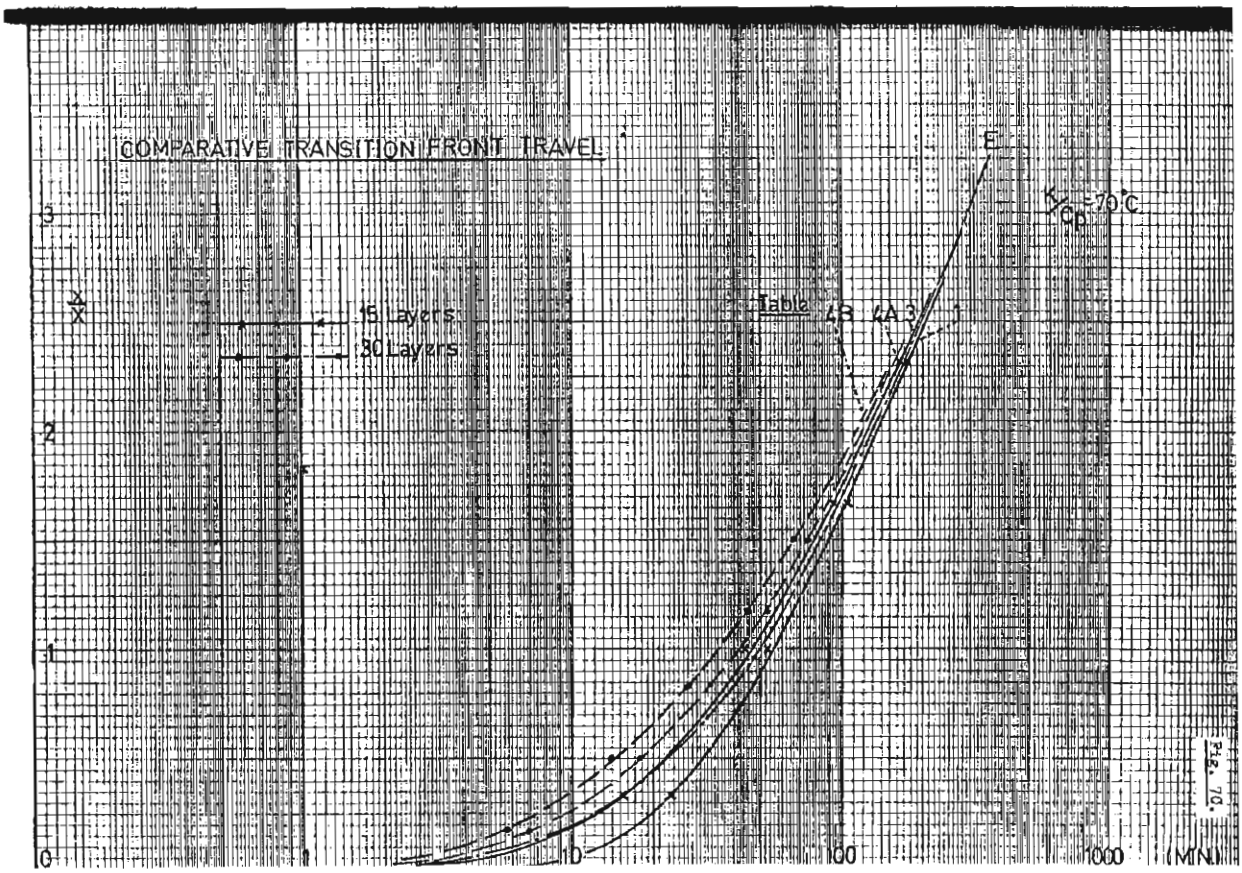
COMPARATIVE TRANSITION FRONT TRAVEL
E
$K_{/Cp}$ = 70 °C
15 Layers
30 Layers
Table 4B 4A 3 1
Fig. 70.
0
1
2
3
10
100
1000
(MIN.)

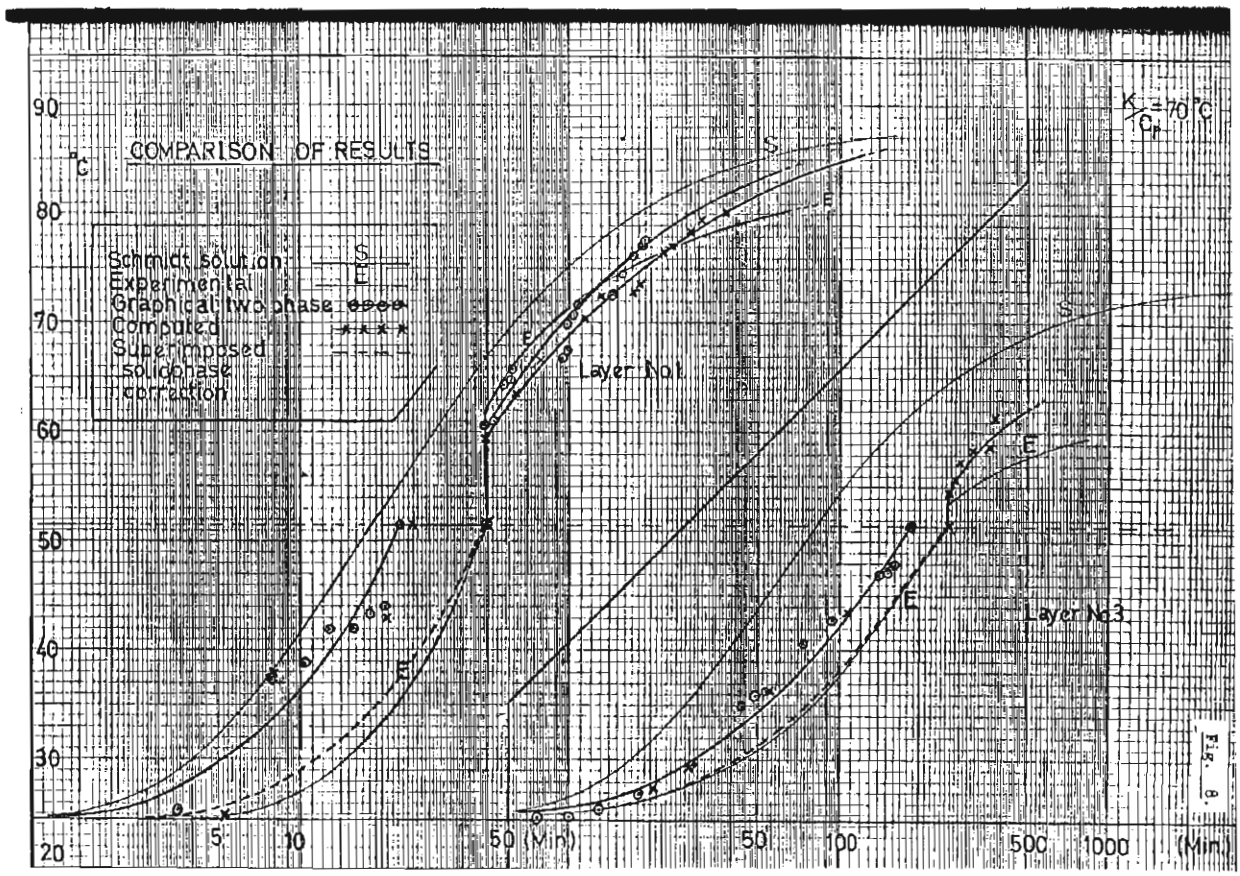
COMPARISON OF RESULTS
°C
$K_{/Cp}$ = 70 °C
Schmidt solution
Experimental
Graphical two phase
Computed
Superimposed
Solidphase correction
S
E
Layer No1
Layer No.3
Fig. 8.
90
80
70
60
50
40
30
20
5
10
50 (Min)
50
100
500
1000
(Min.)

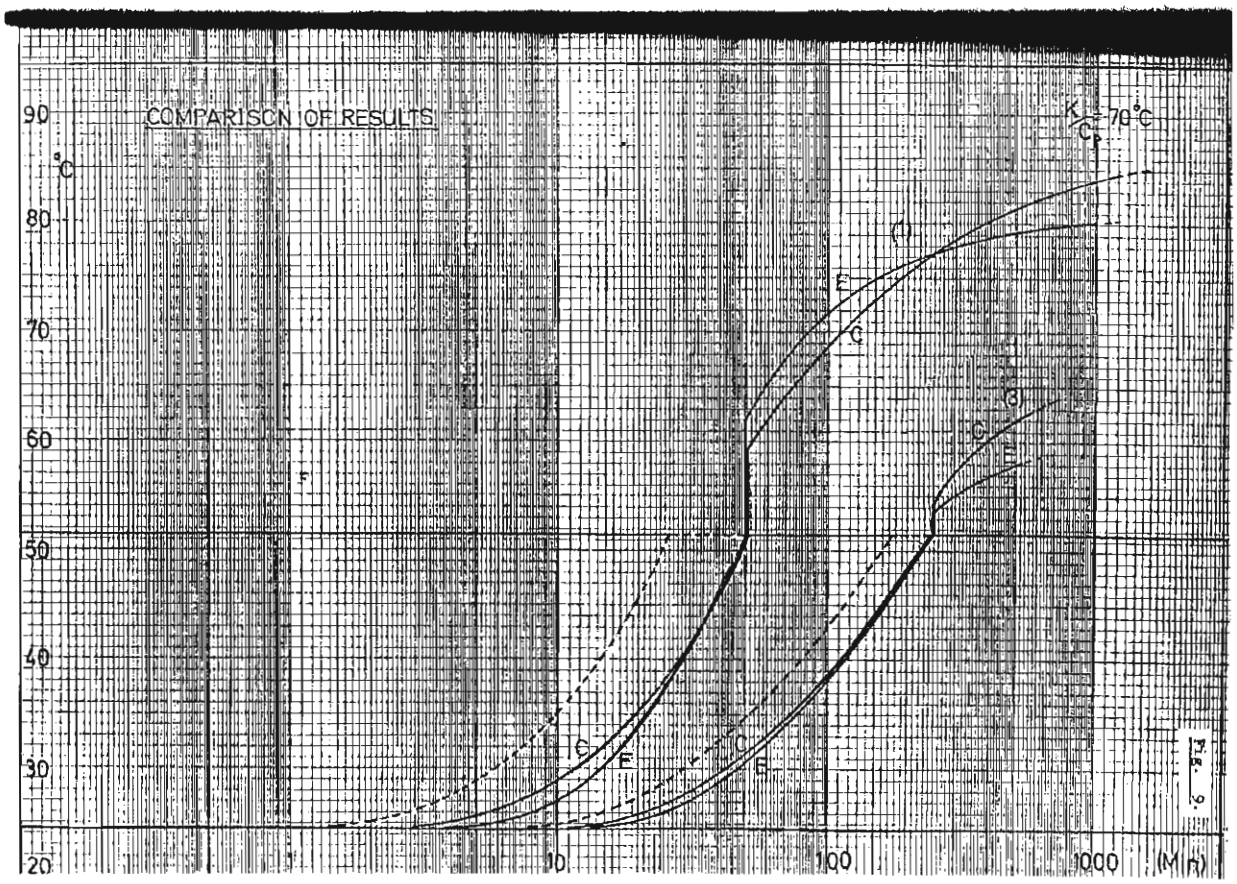
COMPARISON OF RESULTS
°C
90
80
70
60
50
40
30
20
1
10
100
1000
(Min)
K/Cp = 70°C
(1)
(2)
(3)
E
C
F
B

Fig. 9.

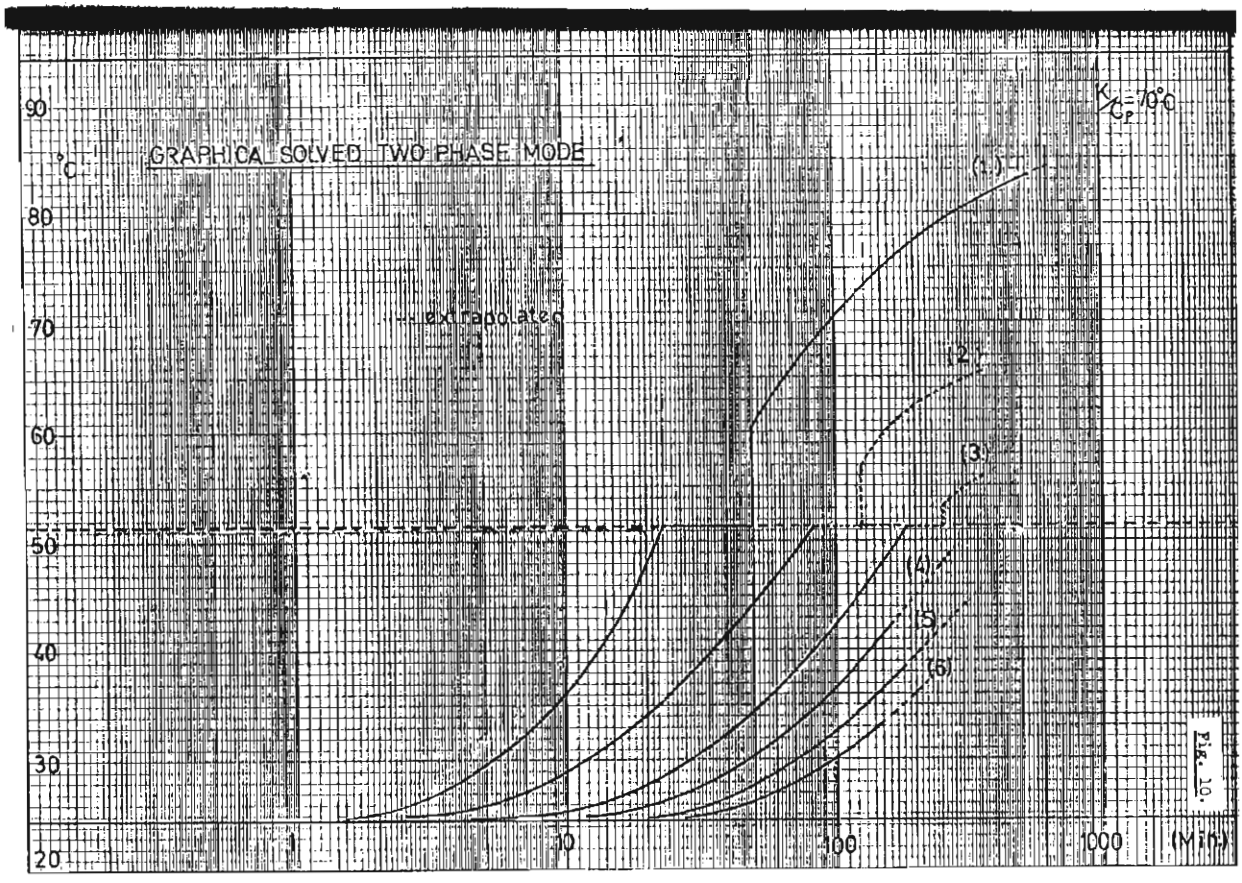
GRAPHICAL SOLVED TWO PHASE MODE
°C
90
80
70
60
50
40
30
20
1
10
100
1000
(Min)
K/Cp = 70°C
--- extrapolated
(1)
(2)
(3)
(4)
(5)
(6)

Fig. 10.

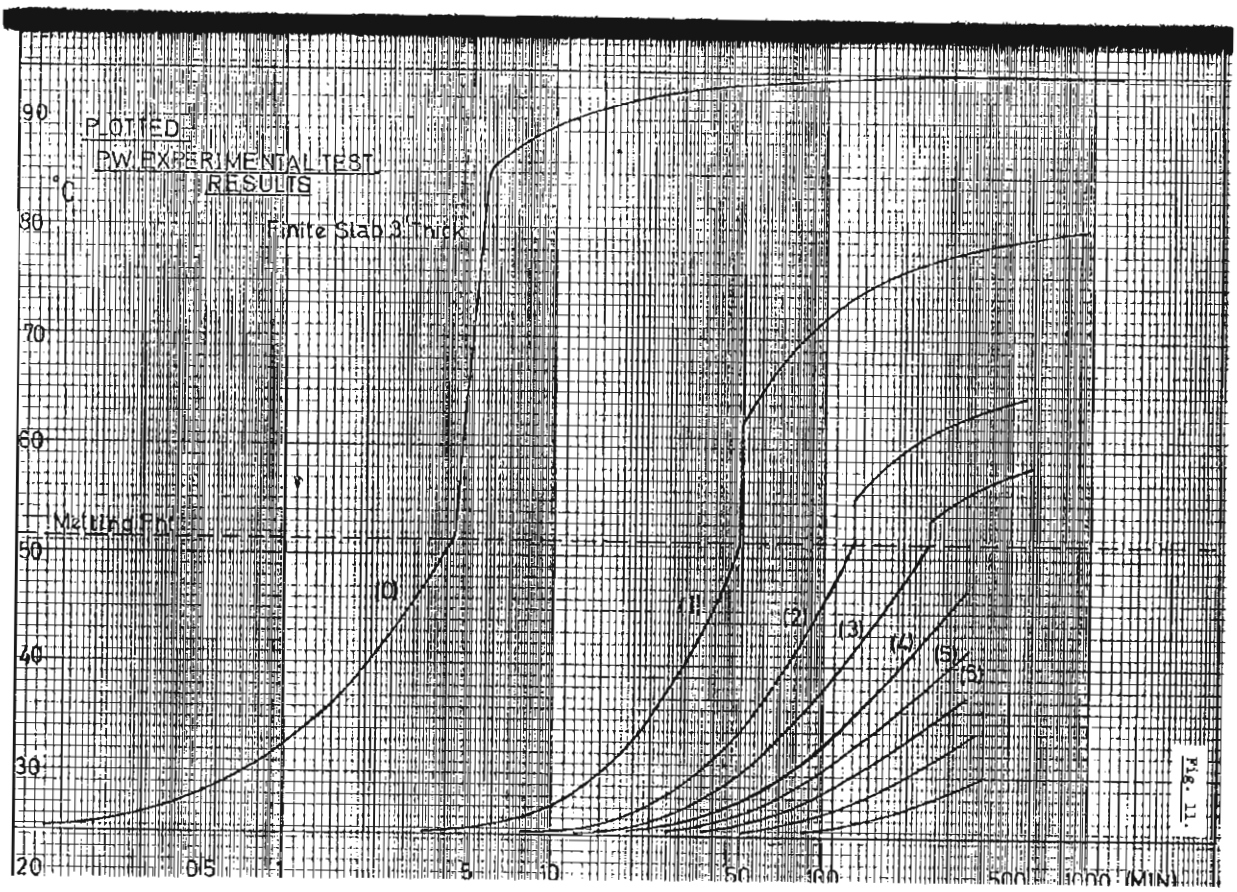
PLOTTED
P.W. EXPERIMENTAL TEST
RESULTS
°C
Finite Slab 3" Thick
Melting Point
(0)
(1)
(2)
(3)
(4)
(5)
(6)
90
80
70
60
50
40
30
20
0.5
1
5
10
50
100
500
1000 (MIN)

Fig. 11.

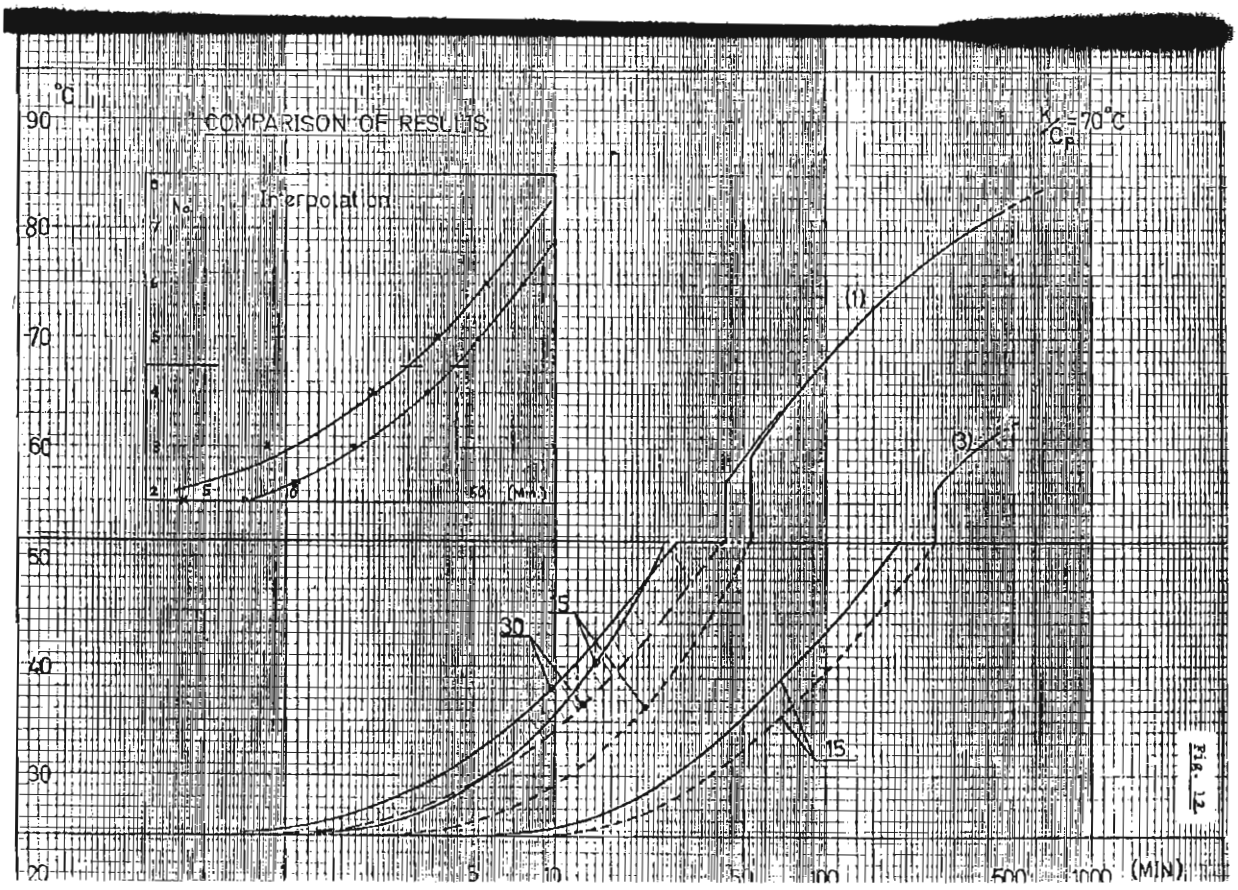
°C
COMPARISON OF RESULTS
Interpolation
(1)
(3)
5
30
15
90
80
70
60
50
40
30
20
5
10
50
100
500
1000 (MIN)

Fig. 12

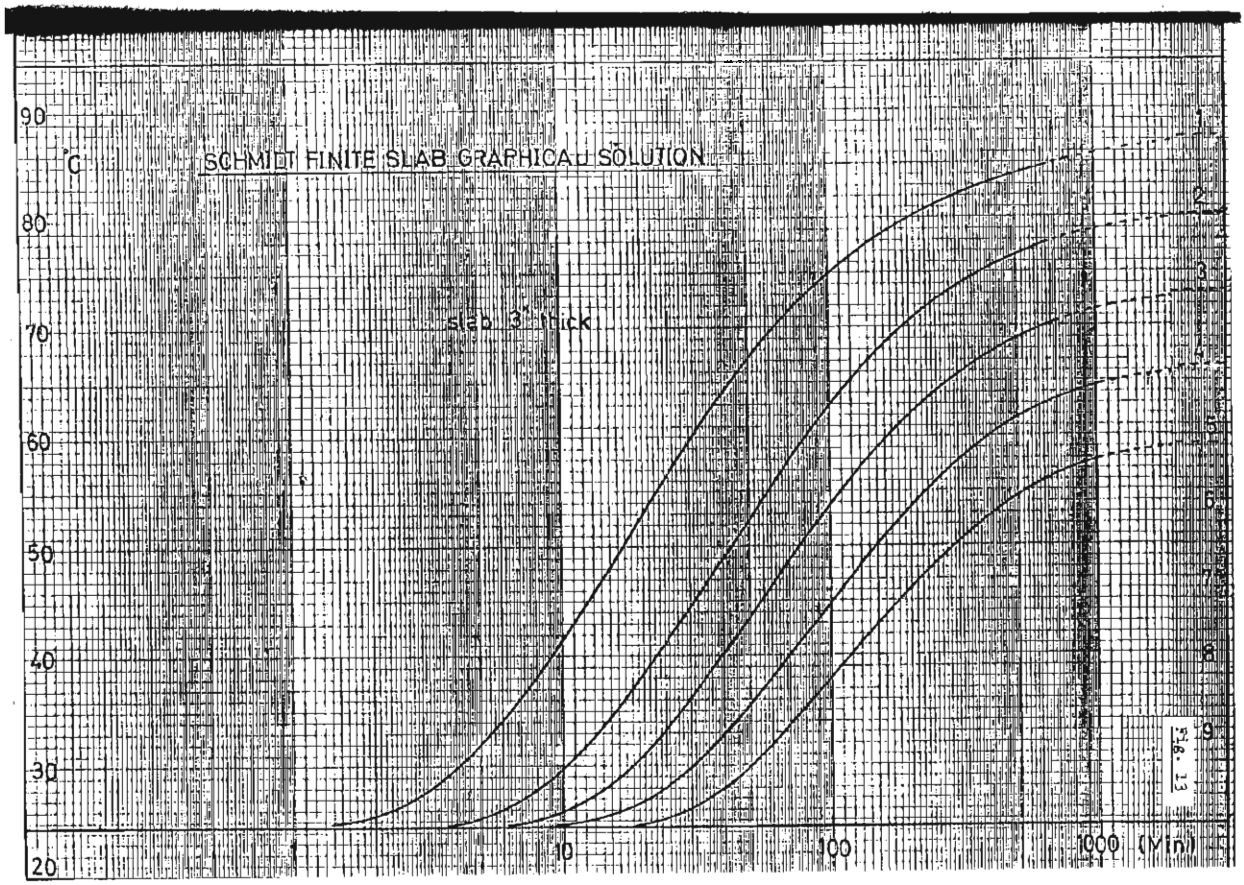
SCHMIDT FINITE SLAB GRAPHICAL SOLUTION
°C
90
80
70
60
50
40
30
20
slab 3" thick
1
10
100
1000 (Min)
Fig. 13

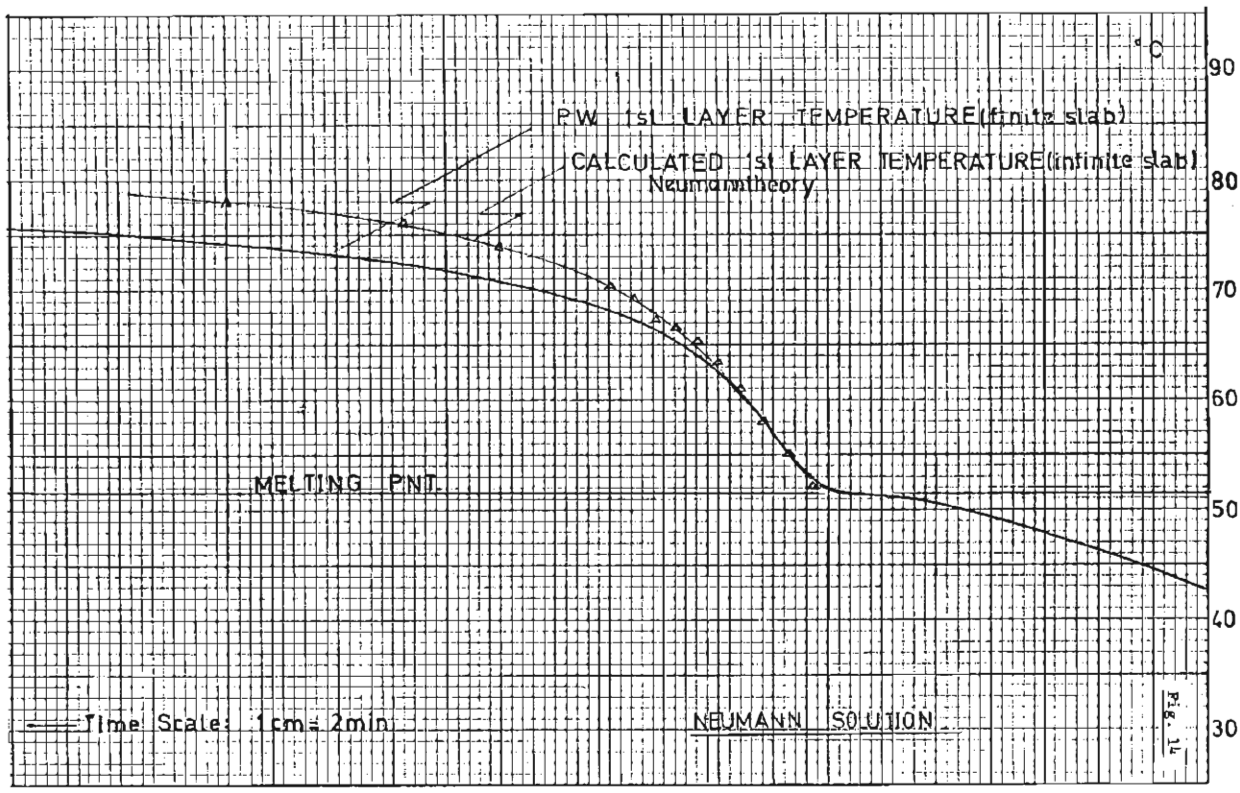
°C
90
80
70
60
50
40
30
P.W. 1st LAYER TEMPERATURE(finite slab)
CALCULATED 1st LAYER TEMPERATURE(infinite slab)
Neumann theory
MELTING PNT.
Time Scale: 1cm = 2min
NEUMANN SOLUTION
Fig. 14

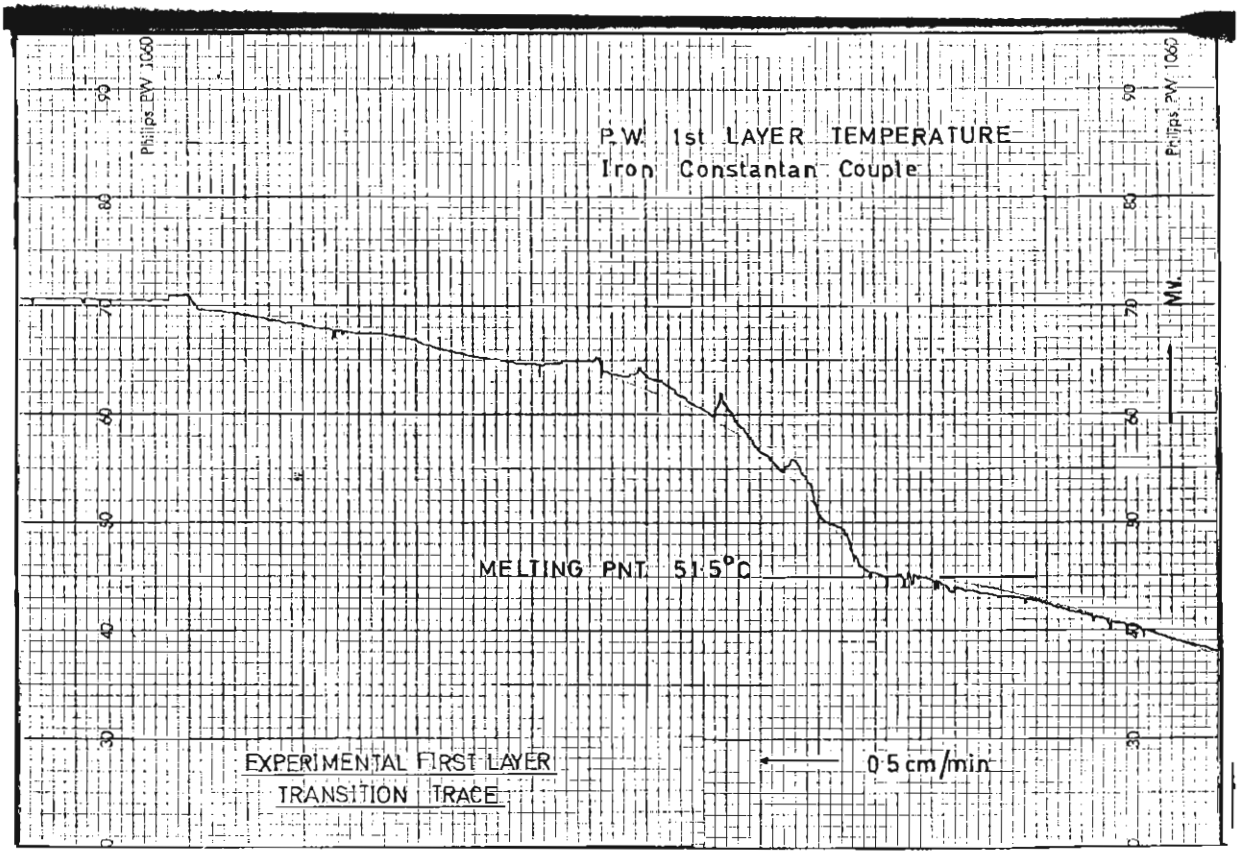
P.W. 1st LAYER TEMPERATURE
Iron Constantan Couple
MELTING PNT 51·5°C
EXPERIMENTAL FIRST LAYER
TRANSITION TRACE
0·5 cm/min
Mv.
Philips PW 1060

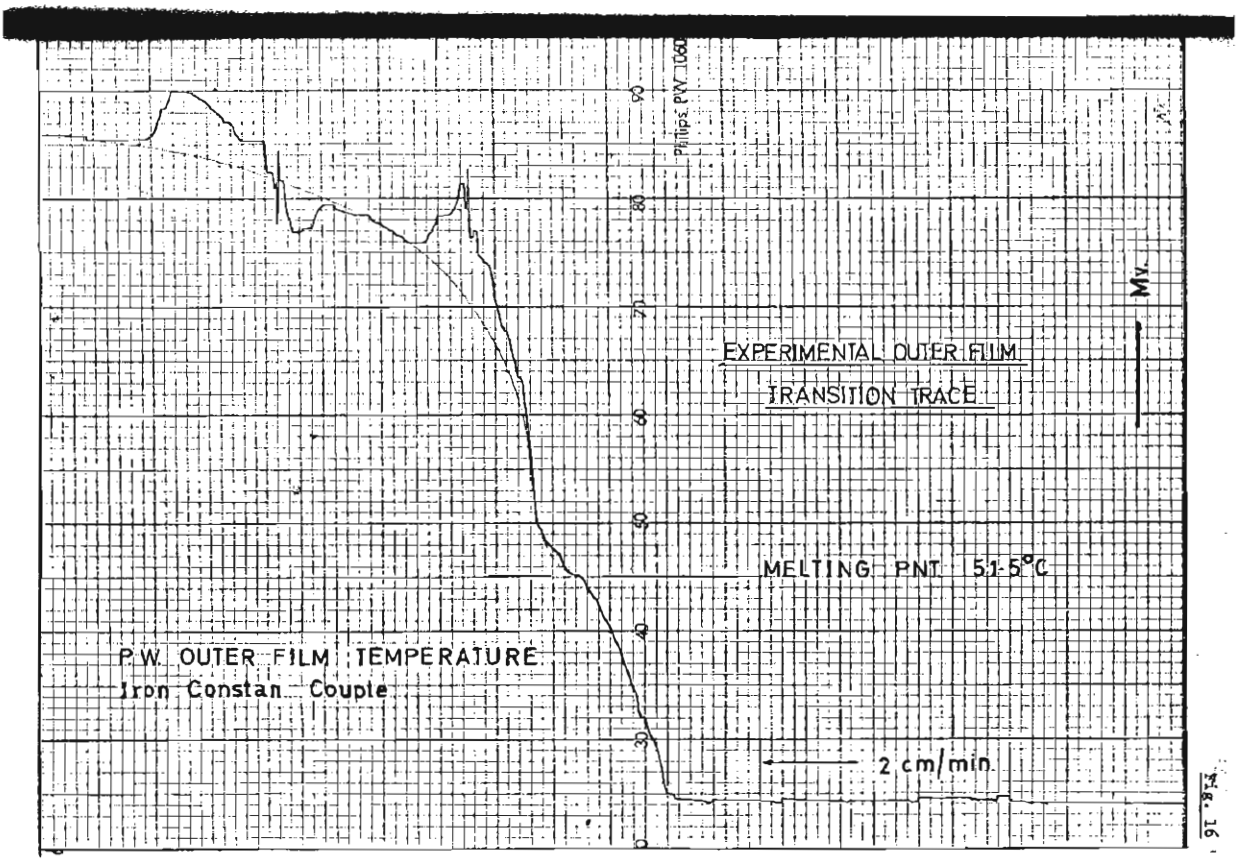
EXPERIMENTAL OUTER FILM
TRANSITION TRACE
MELTING PNT 51·5°C
P.W. OUTER FILM TEMPERATURE
Iron Constan Couple
2 cm/min
Mv.
Philips PW 1060

Fig. 16

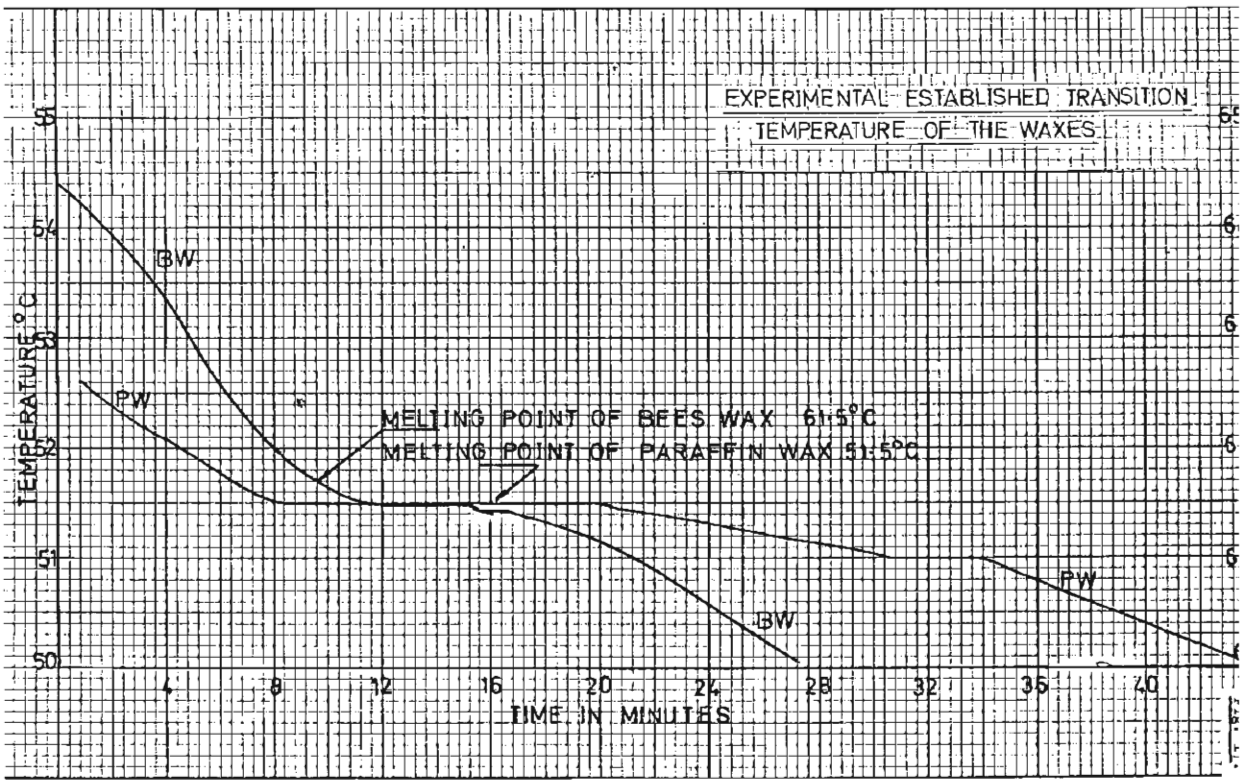
EXPERIMENTAL ESTABLISHED TRANSITION
TEMPERATURE OF THE WAXES
TEMPERATURE °C
55
54
53
52
51
50
BW
PW
MELTING POINT OF BEES WAX 61·5°C
MELTING POINT OF PARAFFIN WAX 51·5°C
PW
BW
4
8
12
16
20
24
28
32
36
40
TIME IN MINUTES

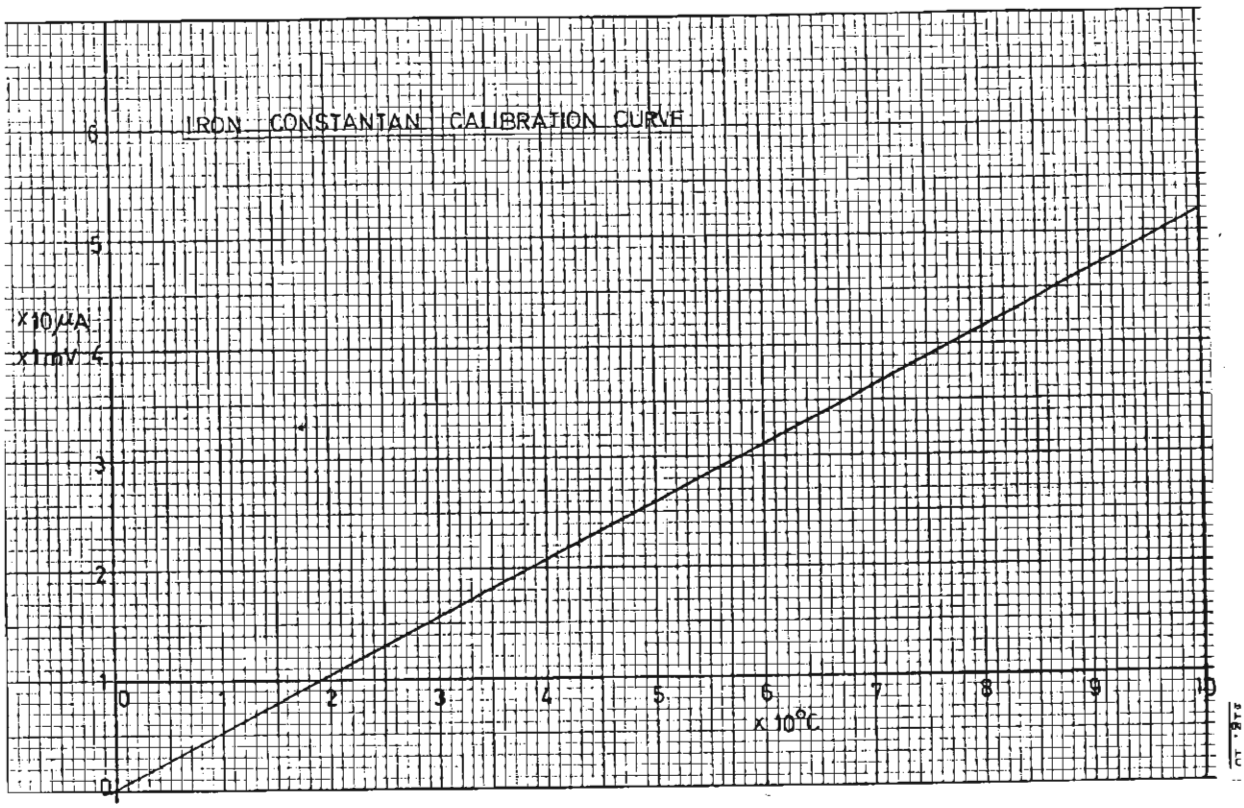
IRON CONSTANTAN CALIBRATION CURVE
x10 μA
x1mV
6
5
4
3
2
1
0
0
1
2
3
4
5
6
7
8
9
10
x 10°C

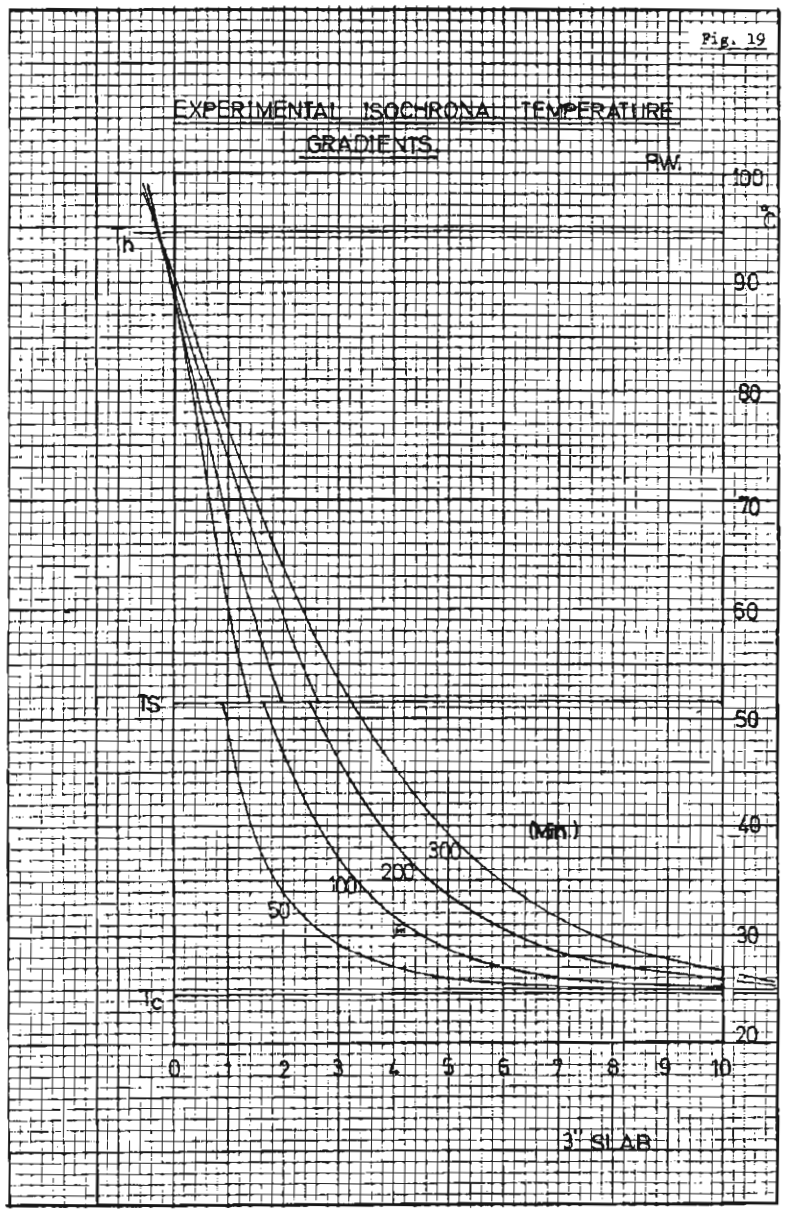
Fig. 19
EXPERIMENTAL ISOCHRONAL TEMPERATURE GRADIENTS.
B.W.
h
TS
Tc
300
200
100
50
(Min)
0 1 2 3 4 5 6 7 8 9 10
3" SLAB
100 90 80 70 60 50 40 30 20

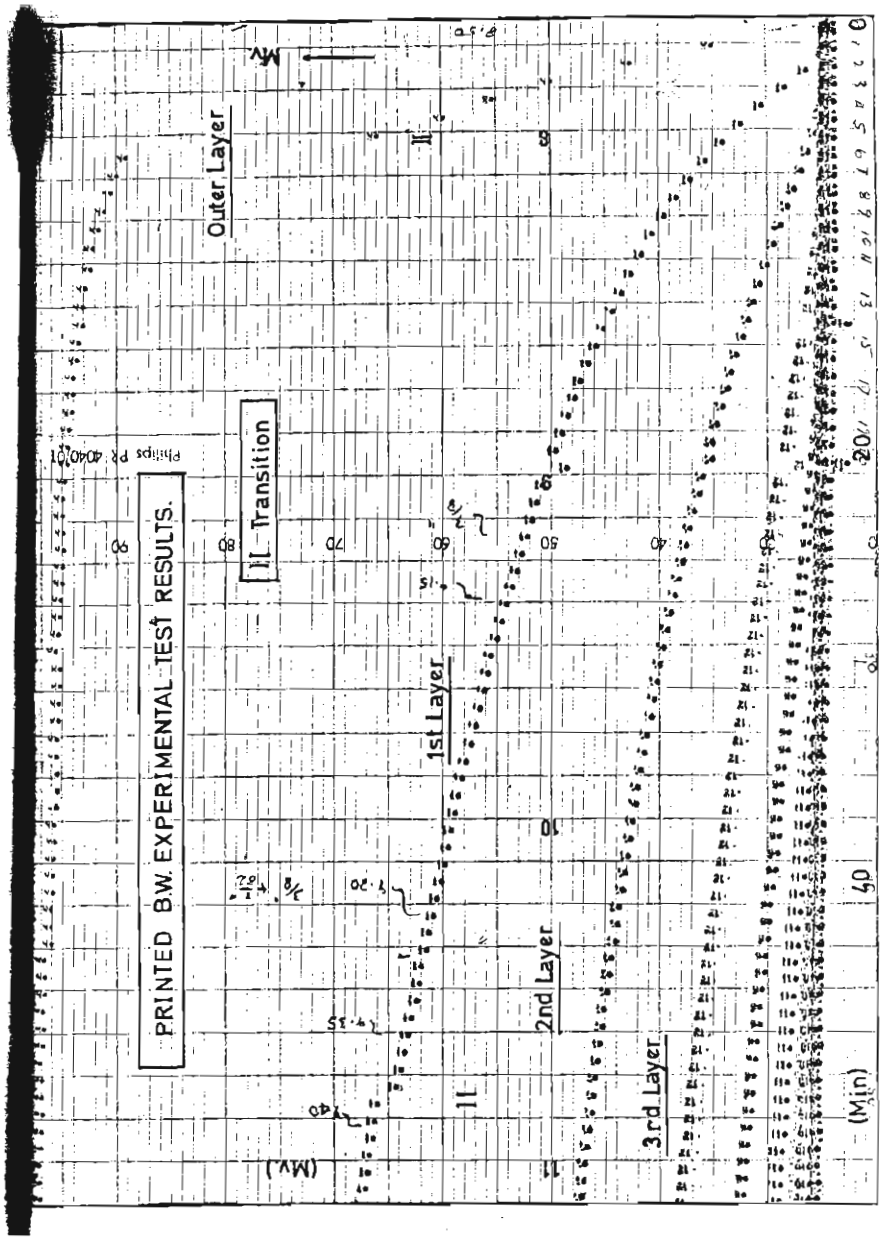
PRINTED B.W. EXPERIMENTAL TEST RESULTS.
Outer Layer
II Transition
1st Layer
2nd Layer
3rd Layer
(MV)
(Min)

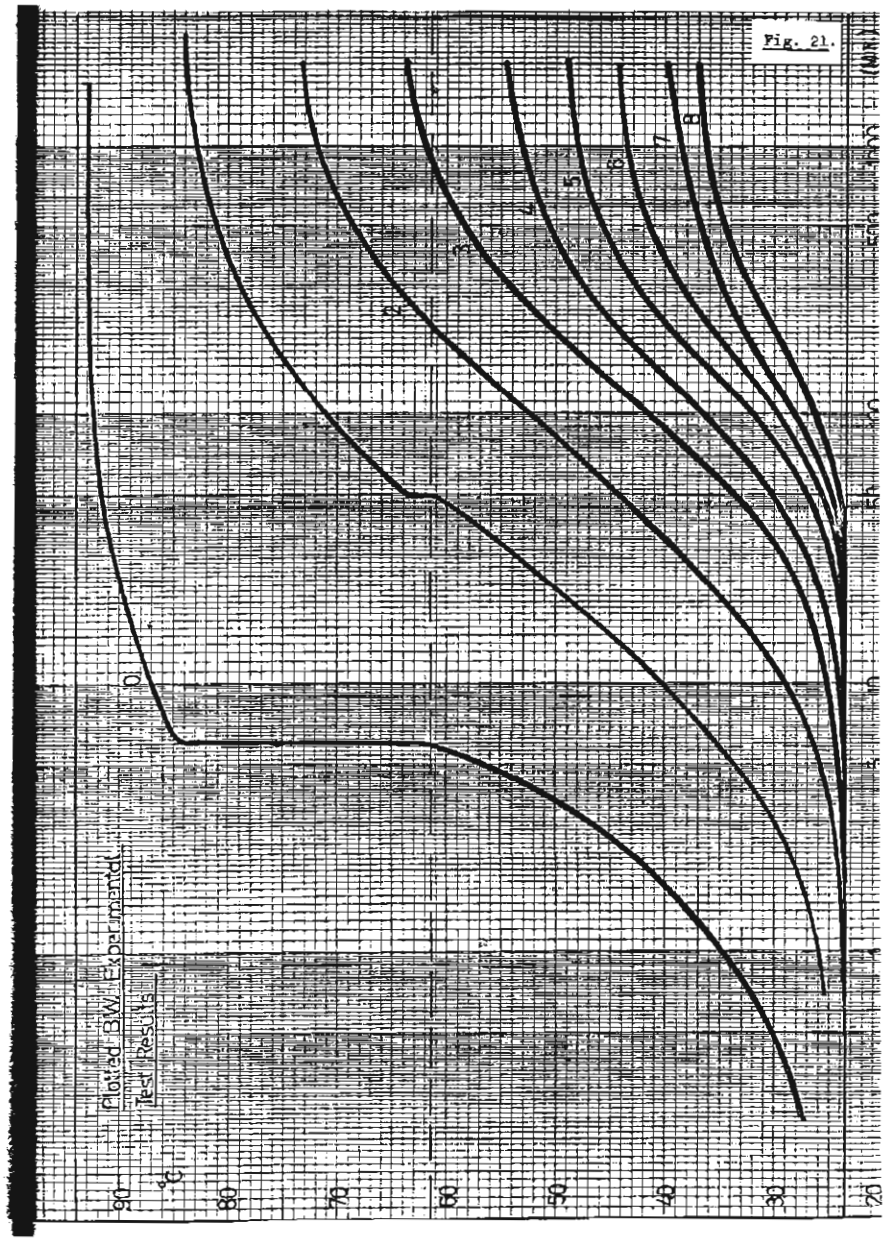

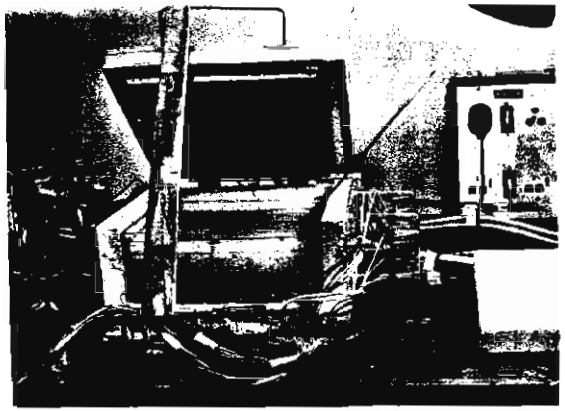

PLATE 1

APPARATUS WITH HEATING PLATE REMOVED.

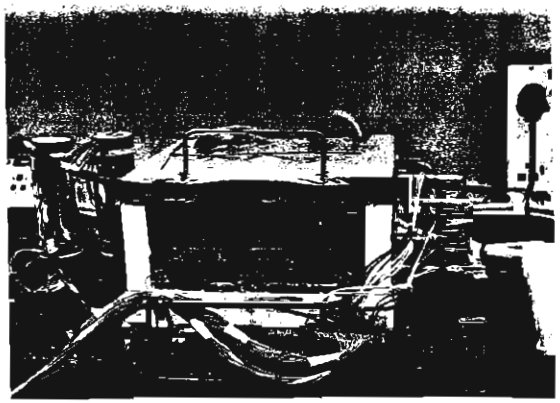

APPARATUS WITH HEATING PLATE IN POSITION.

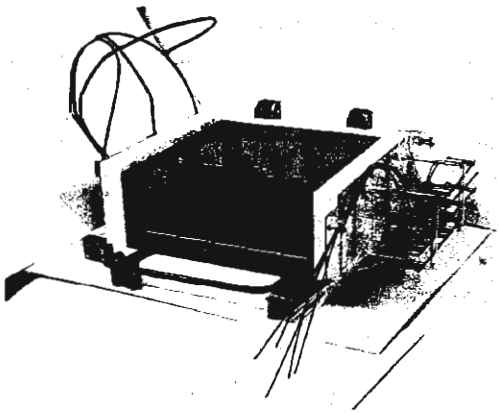

PLATE 2.

LAYOUT OF THERMOCOUPLES IN EXPERIMENTAL WAX MODEL.

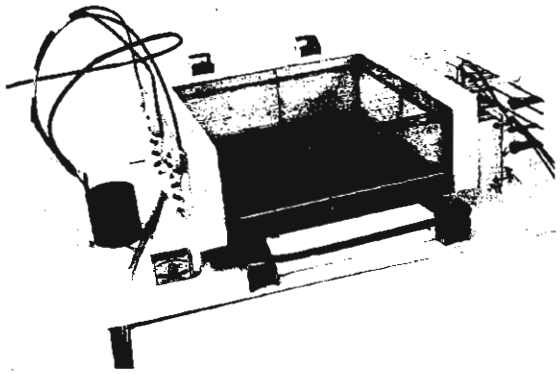

PLATE 3.

LAYOUT OF THERMOCOUPLES IN EXPERIMENTAL WAX MODEL.

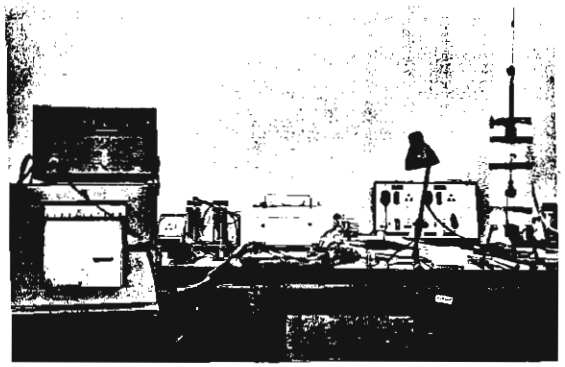

PLATE 4.

EXPERIMENTAL LAYOUT OF WAX MODEL WITH FRONT INSULATION COVER.

EXPERIMENTAL LAYOUT OF WAX MODEL WITHOUT FRONT INSULATION COVER.

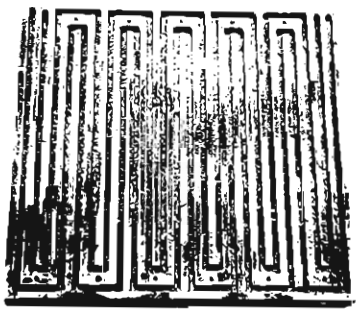

a.

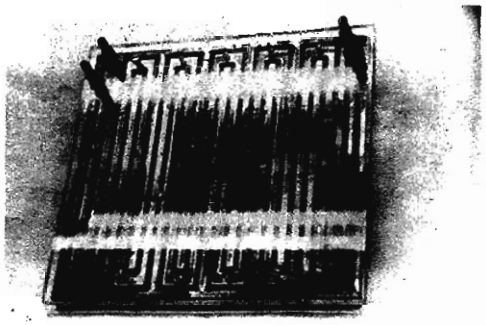

b.

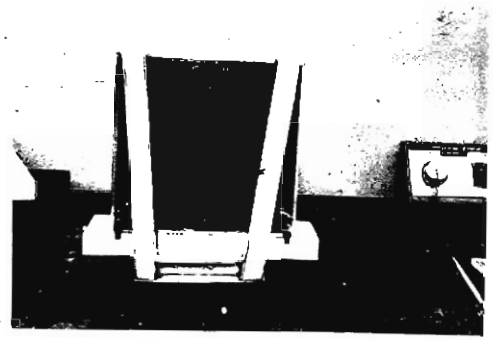

c.

PLATE 5.

a. HEATING/COOLING PLATE MACHINED.

b. HEATING/COOLING PLATE WITH PERSPEX COVER

c. COOLING PLATE MOUNTED.

APPENDIX. A.

EXPERIMENTAL WORK

1. DESIGN OF THE APPARATUS

GENERAL:

The basis of the design of the experimental apparatus has been to simulate the general boundary conditions for analytical and numerical solutions for unsteady state heat transfer, which can be solved rapidly and employed as a basis of correlation. This is the temperature step hypothesis of the heating or cooling source when the material is at uniform temperature.

A heat transfer material was selected with a relatively low phase change temperature range to simplify the apparatus construction, subsidiary equipment, and experimental procedures.

DISCUSSION: The general Fourier equation for transient heat conduction in three dimensions is:

$$\frac{\partial \phi}{\partial \tau} = a \nabla^2 \phi + \frac{Q'''}{\rho C_p}$$

where: ϕ - Temperature excess

∇ - Differential operator $= \frac{\partial}{\partial x} + \frac{\partial}{\partial y} + \frac{\partial}{\partial z}$

Q''' - Heat produced or withdrawn/unit volume

a - Heat transmissivity of the material

Eliminating the y and z components, the equation is simplified to one dimension, or physically, an infinite slab of finite thickness.

Hence the equation becomes

$$\frac{\partial \phi}{\partial \tau} = a \frac{\partial^2 \phi}{\partial x^2} + \frac{Q'''}{\rho C_p}$$

The step function boundary conditions becomes

$$T = T_0 \quad , \tau = 0$$

$$T = T_1 \quad , \tau < 0$$

where T_0 refers to a uniform ambient temperature of the heat transfer material and the heating and cooling surfaces, and T_1 the constant

o/

Temperature change within the material is measured with equally spaced longitudinal welded iron/constantan thermocouples (fig. 1) of negligible heat capacity, the diameter being only a few thousands of an inch, stretched perpendicularly to the direction of heat flow across the material with the junction in the centre. This proved to be a very satisfactory arrangement. Elongation due to temperature change is compensated for by means of spring loaded suspension at the one end with elastic bands arranged in a array.

Thermocouples were also included to measure possible temperature gradients perpendicular to the direction of heat flow because of finiteness off the wax slab.

The result came to be a sophisticated experimental arrangement which produced very accurate experimental results with a reproducability of better than 95%.

Compare the systematic sketch (fig. 1) and photographs.

2. INSTRUMENTATION.

Initially a multichannel high speed oscillograph recorder was employed, but due to the low thermal time response of the experimental arrangement, this method was abandoned. An ordinary multipoint print recorder was then used, augmented by a single channel continuous recorder to capture the thermal transition phenomena of phase change (fig. 15 and 16) from solid to liquid at the different positions in the material.

This arrangement gave very satisfactory recordings; the point recorder showed clearly the heating to equilibrium of the layers divided by the thermocouples as well as the phase transition, and the continuous recorder the details of the transitions.

Recordings are included in this report (fig. 4 and 20 - multipoint recording and fig. 15 and 16 single point continuous recording.)

The zero point was pure melting ice.

To measure the temperatures of the heating and cooling plates and

to determine temperature gradients over its surface, thermocouples were imbedded into the contact surface of the material; four on the heating plate and three on the cooling plate.

3. EXPERIMENTAL PROCEDURES.

The apparatus is initially cooled throughout to thermal equilibrium by circulating water at constant temperature through both the heating and cooling plates. The top (heating) plate is then removed and coupled to a saturated steam supply. When this heating unit has obtained the temperature of the condensing steam throughout, it is placed into position on the apparatus whereupon heating of the wax commences according to the temperaturestep of the heating. The output of all the thermocouples are recorded and experimental conditions sustained until equilibrium is achieved or conditions nears equilibrium. After cooling the test can be repeated to determine repetition accuracy.

4. EXPERIMENTAL RESULTS :

Results have been obtained for paraffin wax (PW) as well as bees wax (BW). The printed experimental results have been plotted on a logarithmic scale and is shown in fig. 11 and fig. 7A. The printed transition phenomena for P.W. is also shown in fig. 21.

Continuous recorded transition traces is shown in fig. 15 and fig. 16 for the outer layer (o) and 1st layer (1) respectively.

BASIC SCHMIDT METHOD - UNSTEADY STATE HEAT CONDUCTION IN A THERMAL HOMOGENEOUS MATERIAL

The general Euler equation for heat conduction for a volume element is given by

$$\frac{\partial T}{\partial \tau} = a\nabla^2 (T) + Q'''$$

where the symbols denote the following:-

T - temperature

τ - time

∇ - operator $\frac{\partial}{\partial x} + \frac{\partial}{\partial y} + \frac{\partial}{\partial z}$

Q''' - heat generated/unit volume

a - thermal diffusivity

For one-dimensional thermally homogeneous material the equation becomes

$$\frac{\partial T}{\partial \tau} = a\frac{\partial^2 T}{\partial x^2}$$

being a linear second order partial differential equation. In Schmidt's solution finite layers or slabs are considered and consequently the relationship becomes

$$\frac{\Delta T}{\Delta \tau} = a\frac{\Delta^2 T}{\Delta x^2}$$

which can be rearranged to

$$\frac{\Delta T}{\Delta \tau} = \frac{\Delta(\Delta T)}{(\Delta x)^2}$$

and multiplying by $\Delta\tau$ and rearranging again

$$\Delta T = a\frac{\Delta \tau}{(\Delta x)^2}\Delta(\Delta T)$$

Substituting $\frac{a\Delta\tau}{(\Delta x)^2} = \frac{1}{2}$, a graphical constant,

$$\Delta T = \tfrac{1}{2}\Delta(\Delta T) \quad \text{---} (1)$$

2/.....

and for a series of layers m and time interval n

$$T_{m,n} = \tfrac{1}{2}(t_{m-1,n-1} + t_{m+1,n-1})$$

which is the arithmetic mean of the temperatures previously prevailing at sections (m - 1) & (m + 1). The same conclusion is made if a heat-balance on a slab is considered. (3)

Various boundary conditions can be evaluated and is rapidly derived by means of a heat balance (1), (2) and (3). In this discussion a constant temperature fluid and convection coefficient will be used to cool a heated block.

The heat flow is represented by

$$q = k\left(\frac{\Delta T}{\Delta x}\right)_w$$

$$q = h(T_w - T_f)$$

$$\text{eg. } \left(\frac{\Delta T}{\Delta x}\right)_w = \frac{h}{k}(T_w - T_f)$$

and when T = 0

$$\left(\frac{\Delta T}{\Delta x}\right)_w = \frac{h}{k}(T_w - T_f)$$

or

$$\left(\frac{\Delta T}{\Delta x}\right)_w = \frac{T_w - T_f}{k/h}$$

The interpretation of the latter relationship is the tangential intersection distance of the graphical formulation as to initial temperature See also figure 3.

3/ ....

Fig.

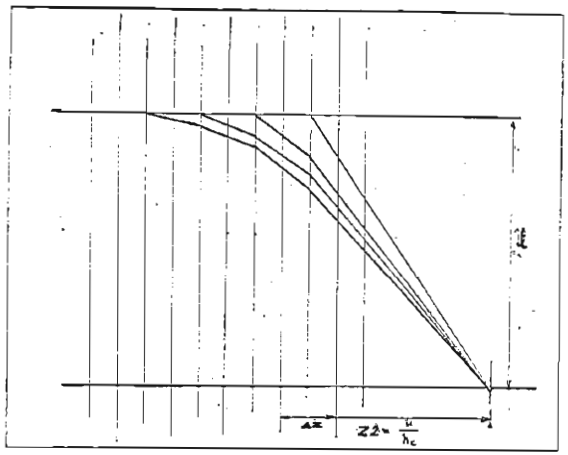

APPENDIX C.

Dimensional analysis of the Fourier heat condution equation.

$$\frac{\partial T}{\partial \tau} = a \nabla^2 T + \frac{\dot{Q}'''}{\rho C_p}$$

$$\left[\frac{\partial T}{\partial \tau}\right] = \left[\frac{T}{\tau}\right]$$

$$a\nabla^2(T) = \frac{k}{\rho C_p}\left(\frac{\partial^2 T}{\partial x^2} + \frac{\partial^2 T}{\partial y^2} + \frac{\partial^2 T}{\partial z^2}\right)$$

$$\left[a\nabla^2 T\right] = \left[\frac{Q \times L}{L^2 \times \tau \times \Theta}\right] \times \left[\frac{L^3}{M}\right] \times \left[\frac{M\Theta}{Q}\right] \times \left[\frac{\Theta}{L^2}\right]$$

$$= \left[\frac{\Theta}{\tau}\right]$$

$$\left[\frac{\dot{Q}'''}{\rho C_p}\right] = \left[\frac{Q}{L^3 \times \tau}\right] \times \left[\frac{L^3}{M}\right] \times \left[\frac{M\Theta}{Q}\right] = \left[\frac{\Theta}{\tau}\right]$$

i.e. the equation is dimensionally homogeneous

$$\frac{\partial \Theta}{\partial \tau} = a\nabla^2 \Theta + \frac{K'''}{\rho C_p}$$

$$\left[\frac{\partial \Theta}{\partial \tau}\right] = \left[\frac{\Theta}{\tau}\right]$$

$$\left[a\nabla^2 T\right] = \left[\frac{\Theta}{\tau}\right]$$

$$\left[\frac{\dot{Q}'''}{\rho C_p}\right] = \left[\frac{Q}{M \times \tau}\right] \times \left[\frac{M \times \Theta}{Q}\right] = \left[\frac{\Theta}{\tau}\right]$$

Hence the dimensional homogeneity of this form of the equation is also proved.

APPENDIX D.

a. Gauss Error-Function solution for simple transient heat conduction [4],[5].

It can be shown that the DE.

$$\frac{\partial \phi}{\partial \tau} = \alpha \frac{\partial^2 \phi}{\partial x^2}$$

with boundary conditions $\left.\begin{matrix} (\phi = o,\ \tau \geq o) \\ (\quad\quad\quad\quad) \\ (\phi = \phi_o,\ \tau \geq o) \end{matrix}\right\} x = o$

is satisfied by the equation

$$\phi = \phi_o \ 1 - G(z) \qquad ---(1)$$

where

$$G(z) = \frac{2}{\sqrt{\pi}} \int_o^z e^{-z^2} \cdot dz \qquad ---(2)$$

$$z = \frac{x}{\sqrt{4\alpha\tau}} \qquad ---(3)$$

G(z) is the Gaus Error Function, or Probability Integral of statistics, for z and equation (3) gives the relationship between z, x, α, τ; where $z = f(x,\tau)$, α = constant.

Equation (2) can be expanded in a power series and becomes,

$$G(z) = \frac{2}{\sqrt{\pi}} \left(z - \frac{z^2}{113} + \frac{z^5}{215} - \frac{z^7}{317} + \quad \ldots\ldots\right) \qquad ---(4)$$

a function of z only.

Tabulated values of (4) are readily available,[6] and by using (1), (3) and (4), resolves an unique numeric method of solution for unsteadystate heat conduction.

Example of numeric values for (4) HSU p. 70.

z	: o	.02	.04	.06
erf o.z = G(z)	: 0	.02256	.04511	.06762

b. NEUMANN SOLUTION FOR TRANSIENT HEAT CONDUCTION WITH PHASE CHANGE [5].

I. Solidification, x > 0:-

Boundary conditions:

$$t_1 = t_2 = T_1,\ x = \chi(\tau) \qquad ---(1)$$

WHERE (ϕ = temperature excess
(T_1 = transition temperature
(X = transition boundary
(L = heat of formation
(1 = solid, 2 = liquid

a heat balance at X produces,

$$k_1 \frac{\partial \phi_1}{\partial x} - k_2 \frac{\partial \phi_2}{\partial x} = L \frac{dx}{d\tau} \qquad ---(2)$$

and $\phi = f(x,\tau)$, $\phi_1 = T_1 = \phi_2$,

$$d\phi_1 = \frac{\partial \phi}{\partial x} dx + \frac{\partial \phi_1}{\partial \tau} d\tau = 0 \qquad ---(3)$$

$$d\phi_2 = \frac{\partial \phi_2}{\partial x} dx + \frac{\partial \phi_2}{\partial \tau} d\tau = 0 \qquad ---(4)$$

substituting (3) and (4) in (2),

$$k_1 \frac{\partial \phi_1}{\partial x} - k_2 \frac{\partial \phi_2}{\partial x} = -L\rho \frac{\partial \phi_1 / \partial \tau}{\partial \phi_1 / \partial x} = -L \frac{\partial \phi_2 / \partial \tau}{\partial \phi_2 / \partial x}$$

3-dimensional;

$$k_1 \cdot \nabla \phi_1 - k_2 \cdot \nabla \phi_2 = -L\rho \frac{\partial \phi_1 / \partial \tau}{\nabla \phi_1} = -L\rho \frac{\partial \phi_2 / \partial \tau}{\nabla \phi_2}$$

and for linear heat flow,

$$\alpha_1 \frac{\partial^2 \phi_1}{\partial x^2} = \frac{\partial \phi_1}{\partial \tau} \qquad ---(5)$$

$$\alpha_2 \frac{\partial^2 \phi_2}{\partial x^2} = \frac{\partial \phi_2}{\partial \tau} \qquad ---(6)$$

Solutions for ϕ_1 and ϕ_2 are obtained from (5) and (6) in the Error Function form,

$$\phi = \phi_0 \left[1 - G(z) \right] = \phi_0 \left[1 - \text{erfc}.z \right] = \phi_0 \, \text{erf}.z$$

i.e., $\phi_1 = A \, \text{erf}. \dfrac{x}{2(a_1\tau)^{\frac{1}{2}}}$ ---(7)

$$\phi_2 = V - B \, \text{erfc}. \frac{x}{2(a_2\tau)^{\frac{1}{2}}} \qquad \text{---(8)}$$

where A and B are constants

V - excess temperature step, $x = 0$

$\tau \geq 0$

Substitution of (7) and (8) into condition (1);

$\phi_1 = \phi_2 = T_1$

$x = X$

$$A \, \text{erf} \frac{X}{2(a_1\tau)^{\frac{1}{2}}} = V - B \, \text{erfc}. \frac{x}{2(a_2\tau)^{\frac{1}{2}}} = T \qquad \text{---(9)}$$

To solve for A and B, define

$$X = 2\lambda(a_1\tau)^{\frac{1}{2}} \qquad \text{---(10)}$$

where λ - numeric constant.

Hence, from (9):

$$A = \frac{T_1}{\text{erf} \dfrac{x}{2(a_1\tau)^{\frac{1}{2}}}} \qquad \text{---(11)}$$

$$B = \frac{V - T_1}{\text{erfc}.\lambda\left(\dfrac{a_1}{a_2}\right)^{\frac{1}{2}}}$$

and (7) and (8) becomes:

$$\phi_1 = \frac{T_1}{\text{erf}\,\lambda} \, \text{erf} \frac{x}{2(a_1\tau)^{\frac{1}{2}}} \qquad \text{---(12)}$$

$$\phi_2 = V - \frac{V - T_1}{\text{erf}\,\lambda\left(a_1/a_2\right)^{\frac{1}{2}}} \, \text{erfc} \frac{x}{2(a_2\tau)^{\frac{1}{2}}} \qquad \text{---(13)}$$

4/....

λ is determined by using condition (2), and hence substituting

$\dfrac{\partial\phi_1}{\partial x}$, $\dfrac{\partial\phi_2}{\partial x}$, A and B and X from (7), (8), (11) and (10),

respectively, produces

$$\frac{e^{\lambda^2}}{\text{erf}} - \frac{k_1 a_1^{\frac{1}{2}}(V-T_1) e^{-a\lambda^2/a^2}}{k_2 a_2^{\frac{1}{2}} T_2 \, \text{erfc}.\lambda(a_1/a_2)^{\frac{1}{2}}} = \frac{\lambda L \pi^{\frac{1}{2}}}{C_1 T_1} \qquad \text{---(14)}$$

This equation is a function of λ, $e^{-\lambda^2}$, erf λ - $\dfrac{a_1}{a_2}\lambda^2$, erfc λ.

Where k_1, k_2, a_1, a_2, L and T_1 are physical constants, as defined, and V a given boundary condition, solutions for (14) can be calculated, and plotted as a function of λ (5).

In the special case where $k_1 = k_2 =$ and

$$a_1 = a_2 = a$$

equations (12), (13), (14) and (10) simplifies to,

(12): $\phi_1 = \dfrac{T_1}{\text{erf}\,\lambda} \cdot \text{erf} \dfrac{x}{(a\tau)^{\frac{1}{2}}}$ ---(12)'

(13): $\phi_2 = V - \dfrac{V - T_1}{\text{erfc}.\lambda} \, \text{erfc} \dfrac{x}{(a\tau)^{\frac{1}{2}}}$ ---(13)'

(14): $\dfrac{e^{\lambda^2}}{\text{erf}\,\lambda} - \dfrac{(V - T_1)e^{-\lambda^2}}{T_2 \cdot \text{erfc}\,\lambda} = \dfrac{\lambda L \pi^{\frac{1}{2}}}{C T_1}$ ---(14)'

(10): $X = 2\lambda(a\tau)^{\frac{1}{2}}$ ---(10)'

5/ .....

2. Melting, x>0:-

With the boundary condition $V > T_1$, $x > 0$, equations (10), (12), 13, and (14) becomes

$$X = 2\lambda(a_2\tau)^{\frac{1}{2}} \qquad ---(15)$$

$$\phi_1 = \frac{T_1}{\operatorname{erfc} \lambda(a_2/a_1)^{\frac{1}{2}}} \operatorname{erfc} \frac{x}{2(a_1\tau)^{\frac{1}{2}}} \qquad ---(16)$$

$$\phi_2 = V - \frac{(V - T_1)}{\operatorname{erf} \lambda} \operatorname{erf} \frac{x}{2(a_2\tau)^{\frac{1}{2}}} \qquad ---(17)$$

and the equation for the solution of λ,

$$\frac{e^{\lambda^2}}{\operatorname{erf} \lambda} - \frac{\frac{1}{2} a_2^{\frac{1}{2}} T_1 e^{\lambda^2(a_2/a_1)}}{2a_1^{\frac{1}{2}} (V - T_1) \operatorname{erfc} \lambda(a_2/a_1)^{\frac{1}{2}}} = \frac{\lambda L \pi^{\frac{1}{2}}}{C_2(V - T_1)} \qquad ---(18)$$

and again in the special case where

$$K_1 = K_2 = K$$

$$a_1 = a_2 = a$$

(15): $X = 2\lambda(a\tau)^{\frac{1}{2}}$ ---(15)'

(16): $\phi_1 = \frac{T_1}{\operatorname{erfc} \lambda} \operatorname{erfc} \frac{x}{2(a\tau)^{\frac{1}{2}}}$ ---(16)'

(17): $\phi_2 = V - \frac{(V - T_1)}{\operatorname{erf} \lambda} \operatorname{erf} \frac{x}{2(a\tau)^{\frac{1}{2}}}$ ---(17)'

(18): $\frac{e^{\lambda^2}}{\operatorname{erf}\lambda} - \frac{T_1 e^{\lambda^2}}{(V - T_1) \operatorname{erfc} \lambda} = \frac{\lambda L \pi^{\frac{1}{2}}}{C(V - T_1)}$ ---(18)'

3. Calculations

The procedure to find numeric solutions will be as follows:

Step 1: Substitute physical constant into (14) and (18) and solve for λ by means of the group-solution C and J. Fig. 38.

Step 2: Calculate X from (10 and (15)

Step 3: Solve for ϕ_1 and ϕ_2 from (12) & (13),(16) and (17).

APPENDIX . E. NEUMANN SOLUTION SAMPLE CALCULATIONS FOR CORRELATION OF EXPERIMENTAL RESULTS.

To simplify the numeric analysis, the thermal functional constants a taken as constant throughout the temperature range at which the experiments wer conducted, for the liquid as well as the solid phase.

This is infact a reasonable assumption as can be seen in appendix 5 from the summary of numeric values for the thermal constants through different temperature ranges.

For this specific substance the according induced error of working with average values is negligible.

The constant and boundary conditions are;

$L = K = 106$ Btu/lb.

$b = b_1 = b_2 = 0.0842$ Btu/ft.h.°F

$a = a_1 = a_2 = 0.00328$

$C = 0.355$ Btu/lb.h.°F

$T_1 = 51.5 - 24.5 = 27.0$ (°C)

$V = 95 - 24.5 = 70.0$ (°C)

Where the initial temperature, 24.5°C, is taken as the zero referenc

Following, for melting in the region x>0 equations (15) .....(18), appendix 4, becomes:

(15) : $X = 2\,(0.00328)^{\frac{1}{2}}\, \lambda\tau^{\frac{1}{2}}$

(16) : $\phi_1 = V - \frac{V-T_1}{\operatorname{erf} \lambda} \operatorname{erf} \frac{x}{2(0.00328\tau)^{\frac{1}{2}}}$

(17) : $\phi_2 = \frac{T}{\operatorname{erf} e\, \lambda} \operatorname{erf} e \frac{x}{2(0.00328\tau)^{\frac{1}{2}}}$

(18) : $\frac{e^{\lambda^2}}{\operatorname{erf}\lambda} - \frac{C_1 e^{-\lambda^2}}{(V-T_1) \operatorname{erfc} \lambda} = \frac{\lambda L \pi^{\frac{1}{2}}}{C(V-T_1)}$

2/ ....

Substitution of the constant into (16) and solving for λ produces;

$$\frac{e^{\lambda^2}}{\operatorname{erf}\lambda} - \frac{27e^{-\lambda^2}}{(70-27)\operatorname{erfc}} = \frac{\lambda \times 106 \times \pi^{\frac{1}{2}}}{0.555(70-27)}$$

$$\frac{e^{\lambda^2}}{\operatorname{erf}\lambda} - \frac{27e^{-\lambda^2}}{43\operatorname{erfc}\lambda} = \frac{106\,\pi^{\frac{1}{2}}}{0.555 \times 43 \times 1.8}\ \lambda$$

$$\frac{e^{\lambda^2}}{\operatorname{erf}\lambda} - 0.628\ \frac{e^{-\lambda^2}}{\operatorname{erfc}\lambda} = \frac{7.88}{1.0}\ \lambda$$

$$e^{\lambda^2}\operatorname{erfc}\lambda - 0.628\ e^{-\lambda^2}\operatorname{erf}\lambda = 4.36\ \lambda\ \operatorname{erf}\lambda\ \operatorname{erfc}\lambda \quad \text{- (A)}$$

and $\operatorname{erfc}\lambda = (1-\operatorname{erf}\lambda)$ _____ (B)

λ is solved for by progressive itteration by using (A) & (B) and tables (9 for erf λ , until (A) is satisfied.

λ	erf λ	erfc λ	λ^2	e^{λ^2}	$e^{-\lambda^2}$	LH	R
1.0	0.843	0.157	1.0	2.72	0.368	0.232	0.
2.0	0.995	0.005	4.0	54.5	0.0187	0.2603	0.

λ = 1.0: LH = 0.427 - 0.628 x 0.368 x 0.843 = 0.427 - 0.195 = 0.232 →

RH = 7.88 x 1.0 x 0.823 x 0.157 = 1.04 →

λ = 2.0: LH = 0.272 - 0.628 x 0.0187 x 0.995 = 0.272 - 0.0117 = 0.2603

RH = 7.88 x 995 x .005 = 0.0392 →

Fig. Interpolation.

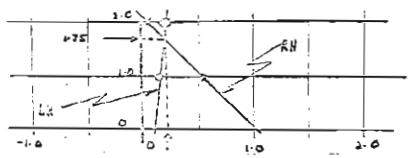

Interpolation for λ resolves λ = 1.8

Hence the functional equations, Appendix 4 page 5, becomes;

(15) : $x = 1.8\ (0.1148)\tau^{\frac{1}{2}} = 0.206\tau^{\frac{1}{2}}$ _____ I

(16) : $\phi_1 = \frac{27}{\operatorname{erfc} 1.75}\ \operatorname{erfc}\ \frac{x}{2(0.0032\tau)^{\frac{1}{2}}}$

$= 2480.0\ \operatorname{erfc}\ \frac{x}{0.1148\tau^{\frac{1}{2}}}$ _____ II

(17) : $\phi_2 = 70 - \frac{43}{\operatorname{erf} 1.75}\ \operatorname{erf}\ \frac{x}{0.1148\tau^{\frac{1}{2}}}$

$= 70 - 43.5\ \operatorname{erf}\ \frac{x}{0.1148\tau^{\frac{1}{2}}}$ _____ III

i.e.

$x = 0.206\tau^{\frac{1}{2}}$ _____ I

$\phi_1 = 2480\ \operatorname{erfc}\ \frac{x}{0.1148\tau^{\frac{1}{2}}}$ _____ II

$\phi_2 = 70 - 43.5\ \operatorname{erf}\ \frac{x}{0.1148\tau^{\frac{1}{2}}}$ _____ III

Because these results are for an infinite thick slab initially at 24.5° (reference 0°C), calculations can only be expected to correlate with initial experimental results, due to the different 2nd boundary condition.

→ Liquid-phase temperature traverse of 1st layer:

→ τ(min)	1	2	3	4	5	6	7
ϕ_2(°C)	51.5	55.06	58.26	61.2	63.54	65.32	66.91

8	9	10	20
67.58	69.67	70.77	78.0

(Fig. 12)

APPENDIX F.

SUMMARY OF FUNCTIONAL CONSTANTS FOR PARAFFIN WAX WHEN USED AS HEAT TRANSFER MATERIAL IN THE EXPERIMENTAL WORK.

Heat Capacity (Cp)	24.5 - 50°C	50 - 70°C	70 - 94.5°C	Average
KCal/Kg°C	0.495	0.525	0.555	0.[illegible]
Btu/lb°F	0.495	0.525	0.555	0.[illegible]
(X1)				
Heat Conductivity (k)				
KCal/m h°C	0.1245	0.1245	0.126	0.1247
Btu/ft h°F	0.08235	0.0835	0.0855	0.082[illegible]
(X 0.672)				
Latent Heat of solution (K)				
KCal/Kg	39 - 59	39 - 59	39 - 59	39 - [illegible]
Btu/lb	70 -106	70 -106	70 -106	70 -[illegible]
(X 1.8)				
Density (ρ)				
Kg/l	0.795	0.78	0.765	0.7[illegible]
lb/ft^3	49.5	48.6	47.7	48.[illegible]
(X 62.4)				
Thermal diffusivity (α)				
(calculated)	0.00340	0.00328	0.00326	0.00[illegible]
dimensionless				
Melting point (°C)				57.5

APPENDIX . G .

Scale factors for graphical solutions.

The following quantities has to be calculated :-

(1) Number and thickness of layers.

The experimental slab is divided into 10 equally spaced layers. In the finite numeric solution, the centre of a layer is the reference (average) temperature. Hence for purposes of comparison, a finite solution comprising 15 layers was executed.

scematically : (also fig ..3..)

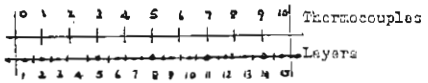

consequently the thickness of each layer $\Delta X = \frac{1 \times 0.167}{12}$ ft

$= 0.0167$ ft.

(2) Time interval.

The value of the time interval for every isochrone is governed by the relation.

$$\alpha \frac{\Delta \tau}{\Delta x^2} = \frac{1}{2}$$

with $\alpha = 0.00328$ and

$\Delta x = 0.025$ ft.

$$\Delta \tau = \frac{1}{2} \times \frac{1}{0.00328} \times (0.0167)^2$$

$= 0.0423$ h

$= 2.54$ min

(3) Locus points for heating and cooling.

The locus points for heating and cooling are found from the experimental results, if the latter is plotted as temperature gradient isochrones on axial fig. ..19.....

The quantity Z_1 , is numeric small, while Z_2 is numeric bigger.

Theoretically $z_2 = \chi_2 = \frac{k}{h_2}$

$$z = \chi_1 = \frac{k}{h_1}$$

is very small, because k, the average conductivity of the wax is small and the h_1, the equivalent connection co-efficient of contact of the wax to the copper plate is large. Subsequently the ratio of k/h will be small.

(4) Heat of transformation and co-efficient $\underline{k}$

The latent heat of solution for the molecular fraction of wax used (melting point 51.5 °C) is given by the scource [4] as 39-59 Kcal/kg, or the equivalent of 70) 106 Btu/lb, for an -phase and - phase respectively. Hence the co-efficient $\underline{k}$ for the - phase becomes

$$\frac{\underline{k}}{c_p} = \frac{70}{0.555} = 126\ ^{\circ}F = 70\ ^{\circ}C$$

The latter value is used in the solution because the temperature axis is in °C.

APPENDIX . H. NUMERIC - RELAXATION SOLUTION METHOD. (7)

The problem is approached through the general Fourier conduction differential equation

$$\frac{\partial t}{\partial \tau} = \alpha \nabla^2 t$$

for three dimensitons and

$$\frac{\partial t_1}{\partial \tau} = a_1 \frac{\partial^2 t_1}{\partial x^2} \qquad \text{--------(1)}$$

$$\frac{\partial t_2}{\partial \tau} = a_2 \frac{\partial^2 t_2}{\partial x^2} \qquad \text{--------(2)}$$

where (1) denotes one-dimensional conduction in the solid state and (2) one-dimensional conduction in the liquid state respectively, where heat transfer is coupled with a change of state of the heat conduction mode.

The heat balance

$$k_1 \left(\frac{\partial t1}{\partial x}\right)_{R^-} = k_2 \left(\frac{\partial t_2}{\partial x}\right)_{R^+} + \rho qs \frac{dR}{d\tau} \qquad \text{---(3)}$$

where k_1, k_2 - solid and liquid state conduction coefficient respectively

t_1, t_2 - solid and liquid state temperature respectively.

ρqs - transition heat

R - transition shift.

gives a relation between (1) and (2).

In this solution (1) is expanded into its finite interval from for solid state evaluation, i.e.

$$\frac{t_{i,\,k+1} - t_{i,\,k}}{t} = \frac{a_1 (t_{i-1,\,k+1} + t_{i+1,\,k+1} - 2t_{i,\,k+1})}{h^2}$$

or

$$-t_{i-1,\,k+1} + (2 + \frac{k^2}{a_1 1}) t_{i,\,k+1} - t_{i+1,\,k+1} = \frac{h^2}{a_1 1} t_{i,}$$

——(

where kl denotes time τ and ih denotes axial distance .

For the liquid state, (2) is transformed by the transformation function

$$\frac{\partial t}{\partial x} = T\,(\tau,\ t(x,\tau)) \qquad \text{------(5)}$$

into

$$\frac{\partial \tau}{\partial \tau} = a_2 \tau^2 \frac{\partial^2 \pi}{\partial t_2^2} \qquad \text{----------(6)}$$

with appropriate partial differentiation and substitution of both (2) and (5 into 3rd power derivitives of t and x and τ.

Evaluating finitely, (6) becomes at the νth itteration.

$$\frac{T_i,^{(\nu)}_{k+1} - T_{i,k}}{l} = \frac{a_2\, T_{i,k+1}^{(\nu-1)\ 2}\ T^{(\nu)}_{i-1,\,k+1} + T_{i+1,\,k+1} - 2T_i,^{(\nu)}_{k+1}}{h^2}$$

or

$$-T_{i-1,\,k+1}^{(\nu)} + \left\{2 + \frac{k^2}{a_2 l\ T_{i,\,k+1}^{(\nu-1)\ 2}}\right\} Ti,^{(\nu)}_{k+1} - T_{i+1,\,k+1}^{(\nu)}$$

$$= \frac{k^2 T_{i,\,k}}{a_2 l\ T_{i,\,k+1}^{(\nu-1)\ 2}} \qquad \text{---------(7)}$$

The latter equations (1) and (2), and (4) and (7) are clearly not linear and are valid only in the bounded range shown in the following figure.

fig.

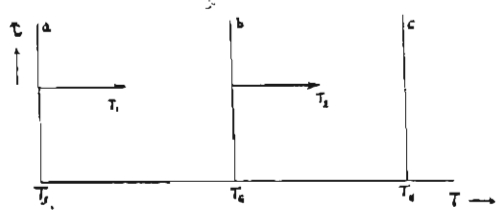

The inverse transformation function T/t is

$$x(t_b) = \int_{ta}^{tb} \frac{dt}{T(\tau,t)} + x(t_a) \qquad \text{---------(8)}$$

Numerical solution.

It is clear that this method does not lend itself to simple evaluation of a physical problem. Solution is done numerically in an array and itterated until the desired degree of accuracy has been obtained - p.671

The authers[7] included calculated solutions computed for the same boundary conditions as in the foregoing demonstrated Neuman analytic solution (App.D) as a basis of correlation from which it is apparent that a decrease in finiteness, decreases the all over macroscopic error.

APPENDIX I. COMPUTER PROGRAM AND PROCEDURE

A - Logic
B - Program

A.

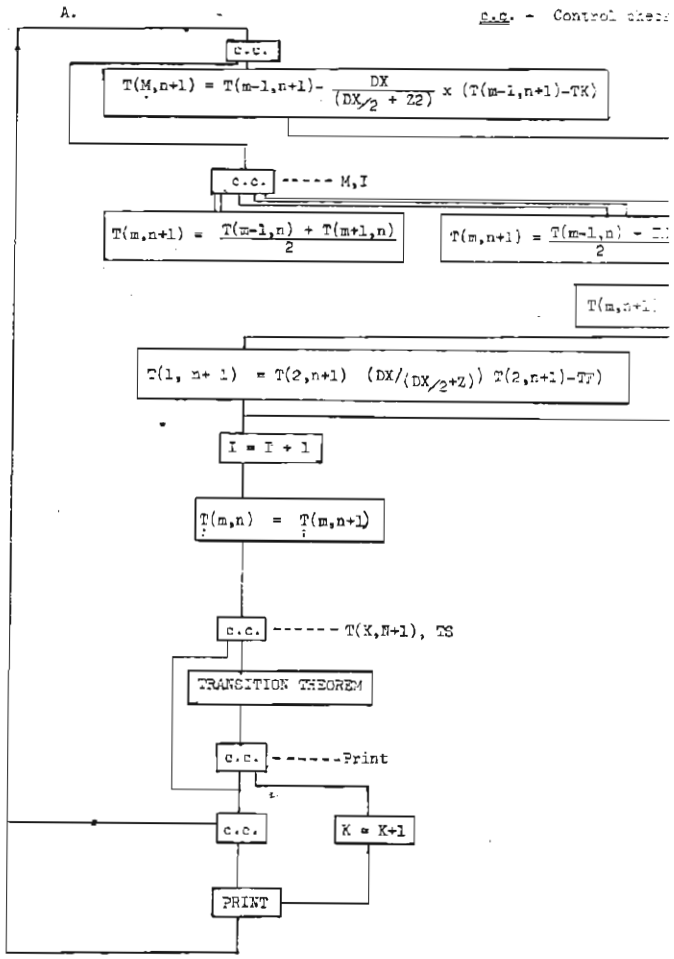

B.

```
16000       DIMENSION T(100,3),TW(3)
16000       READ 1,DX,X,TK,TF,DTY,Z
16032     1 FORMAT(6F10.5)
16125       I=1                          16077       K=1
16133       Z2=1.                        16085       KA=1
16141       II=2                         16093       HEATF=70.
16149       TM=0.                        16101       TS=51.5
16157       T(1,1)=TK                    16109       M=1
16175       T(2,2)=TK                    16117       N=1
16193       TW(1)=TK
16206    52 M=M+1
16219       IF(M-17)70,71,71
16238    71 T(M,N+1)=T(M-1,N+1)-(DX/(DX/2.+Z2))*(T(M-1,N+1)-TK)
16331       GO TO 72
16336    70 IF(M-1)11,16,51
16355    11 T(M,N+1)=(T(M-1,N)+T(N+1,N))/2.
16418       GO TO 52
16423    16 T(M,N+1)=(T(M-1,N)+TK)/2.
16471       GO TO 52
16476    51 T(M,N+1)=TK
16499    72 IJ=M
16507       M=1
16515       T(M,N+1)=T(M+1,N+1)-(DX/(DX/2.+Z))*(T(M+1,N+1)-TF)
16608       TW(N+1)=(T(M,N+1)+T(M+1,N+1))/2.
16671       M=IJ
16679    53 I=I+1
16692       IF(N-2)6,7,7
16711     7 J=M-1
16724       MJ=1
16732       TW(1)=TW(2)
16750       TW(2)=TW(3)
16768    95 T(MJ,1)=T(MJ,2)
16796    96 T(MJ,2)=T(MJ,3)
16824       IF(MJ-J)97,98,15
16843    97 MJ=MJ+1
16856       GO TO 95
16861    98 MJ=MJ+1
16874       GO TO 96
16879     6 N=N+1
16892    15 M=1
16900       IF(K-1)26,26,39
16919    39 IF(T(K,N)-TS)22,21,21
16948    22 GO TO 19
16953    21 KA=KA+1
16966       IF(KA-1)23,23,24
16985    23 T(K,N)=TS
17003       GO TO 63
17008    24 DTM=T(K,N)-TS
17031       TM=TM+DTM
17044       T(K,N)=TS
17062       IF(TM-HEATF)25,26,26
17081    25 GO TO 19
17086    26 K=K+1
17089       TM=0.
17107       KA=0
17115       GO TO 63
17120    19 IF(I-11)52,64,64
17139    64 II=II+10
17152    63 PRINT 99,K,TM,I
17174    99 FORMAT(3F6.1/)
17203       DO2MN=1,IJ
17211     2 PRINT 100,T(MM,2)
17249   100 FORMAT(F6.1,13)
17268       GO TO 52
17273     3 STOP
17280       END
```

APPENDIX. J. DISCUSSION OF COMPUTER PROGRAM.

The computer program, shown in the preceeding section and programmed in FORTRAN-code was used to produce the solutions in the tables section. The calculation of each table was executed independantly.

The numeric value for every tenth temperature isochrone at the centre of the layers is printed out fully as well as the temperature isochrones when transition commences and when transition is completed.

The printed temperature gradients are preceeded by a set of three figures; the 1st denotes the layer which has reached the transition conditions, the 2nd the summed temperature difference TM and the 3rd a counter denoting the No. of the isochrone. Because of programming limitations the printed figure in the 3rd column is I + 1 at the I th interval. Subsequently the table with the summed time intervals are described by the counters I and I + 1. Counting starts at I = 1.

Due to programming, the counter K controlling the transition layer, is printed as K + 1 when transition is completed in that layer.

Time is evaluated from the table of summed time intervals which is calculated for five, fifteen and thirty layers. Time totals are printed adjacent to the corresponding I and I + 1 values. (Table 8)

Computed results are included in tables 1 - 7 and each table is proceeded by the values of the characteristic functions for which the table was computed.